ChemMedChem

Check for updates

Accepted Article

Title: Novel cytotoxic 1,2,3-triazoles as potential new leads targeting the S100A2-p53complex

Authors: Jufeng Sun, Jennifer R Baker, Cecilia C Russell, Peter J Cossar, Hong Ngoc Thuy Pham, Jennette A Sakoff, Christopher J Scarlett, and Adam McCluskey

This manuscript has been accepted after peer review and appears as an Accepted Article online prior to editing, proofing, and formal publication of the final Version of Record (VoR). This work is currently citable by using the Digital Object Identifier (DOI) given below. The VoR will be published online in Early View as soon as possible and may be different to this Accepted Article as a result of editing. Readers should obtain the VoR from the journal website shown below when it is published to ensure accuracy of information. The authors are responsible for the content of this Accepted Article.

FULL PAPER

Targeting the S100A2-p53 interactions with a series of novel 3,5-*bis*(trifluoromethyl)benzene sulfonamides: Synthesis and cytotoxicity

Jufeng Sun,[a,b] Joey I Ambrus, [a] Cecilia C Russell,[a] Jennifer R Baker,[a] Peter J Cossar,[a] Melanie J Pirinen,[c] Jennette A. Sakoff *[d] Christopher J Scarlett,[c] and Adam McCluskey *[a]

[a] Ms J Sun (0000-0002-5165-9396), Dr J Ambrus (0000-0002-9560-301X), Dr CC Russell (0000-0002-4140-7785), Dr JR Baker (0000-0002-9560-301X), Dr PJ Cossar (0000-0002-8260-5710) and Prof A McCluskey (0000-0001-7125-863X)
      Chemistry, School of Environmental & Life Sciences
      The University of Newcastle
      University Drive, Callaghan, NSW 2308, Australia
      E-mail: Adam.McCluskey@newcstle.edu.au
[b] Medicinal Chemistry, School of Pharmacy,
      Binzhou Medical University, Yantai, 264003, China
[c] Ms MJ Predebon (0000-0002-2847-7818) and Prof CJ Scarlett (0000-0002-4140-7785)
      School of Environmental & Life Sciences,
      The University of Newcastle, Ourimbah NSW 2258, Australia.
[d] Dr JA Sakoff (0000-000207009-5792)
      Experimental Therapeutics Group, Department of Medical Oncology
      Calvary Mater Newcastle Hospital
      Edith Street, Waratah NSW 2298, Australia.

      Supporting information for this article is given via a link at the end of the document.

Abstract: *In silico* approaches identified **1**, *N*-(6-((4-bromo-benzyl)amino)hexyl)-3,5-bis(trifluoromethyl)benzene sulfonamide, as a potential inhibitor of S100A2-p53 protein-protein interaction, a validated pancreatic cancer drug target. Subsequent cytotoxicity screening revealed it to be a 2.97 µM cell growth inhibitor of the MiaPaCa-2 pancreatic cell line. This is in keeping with our hypothesis that inhibiting this interaction would have an anti-pancreatic cancer effect with S100A2, the validated PC drug target. A combination of focused library synthesis (3 libraries, 24 compounds total) and cytotoxicity screening identified a propyl alkyl diamine spacer as optimal; the nature of the terminal phenyl substituent had limited impact on observed cytotoxicity, whereas *N*-methylation was detrimental to activity. In total 15 human cancer cell lines were examined, with most analogues showing broad spectrum activity. Near uniform activity was observed against a panel of six pancreatic cancer cell lines: MiaPaCa-2, BxPC-3, AsPC-1, Capan-2, HPAC and PANC-1. In all cases there was good to excellent correlation between the predicted docking pose in the S100A2-p53 binding groove and the observed cytotoxicity, especially in the pancreatic cancer cell line with high endogenous S100A2 expression. This supports S100A2 as a pancreatic cancer drug target.

Introduction

Pancreatic cancer (PC) is one of the most lethal human cancers. This cancer has a depressingly low five-year survival rate of only 7%.[1] It is also projected that pancreatic cancer will be the second leading cause of cancer death by 2030.[2] The highly metastatic nature of PC presents a major challenge for improving patient outcomes. These heterogeneous tumours are composed of cancer cells with differing morphologies and phenotypic profiles, making them extremely difficult to treat as they evade targeted therapies. PC is divided into two main classes: *exocrine tumours* deriving from the cells of the exocrine pancreas and accounting for more than 95% of all pancreatic tumours; and *endocrine tumours* coming from

endocrine cells that produce hormones. Of the two classes, pancreatic ductal adenocarcinoma (PDAC) is the most common cancer subtype, covering about 90% of all exocrine tumours.[3] Current combination chemotherapies for PDAC are highly toxic and only a fraction of patients respond (~30%). As a result, new targeted therapies which are effective against PDAC are urgently needed.

One potentially promising new oncogenic target for the treatment of PC is the S100 calcium binding protein A2 (S100A2), a member of the S100 protein family. S100A2 was first isolated in 1989 and classified as a member of the S100 protein family.[4] Since this time there have been over 25 S100 class protein identified. Of these S100A2 belongs to a highly homologous sub-group that comprises A100A3, S100A4, S100A5 and S100A6.[5-7] The S100A2 gene encodes a protein of 98 amino acid residues, with a molecular mass of ~11 kDa, and is characterised by four helices, two distinct calcium-binding EF-hand motifs, a central hinge region and C- and N-terminal variable domains.[8] Like other S100 proteins, S100A2 occurs as a homodimer *in vitro* and *in vivo*.[6, 7] S100A2 displays a direct interaction with the C-terminal of wildtype p53.[9, 10]

The S100A2 protein forms homodimers and are regulated by Ca^{2+}; this enables the proteins to act as sensors which respond to variations in Ca^{2+} concentrations.[11] The binding of calcium by S100A2 results in the activation of p53 transcriptional activity.[9] S100A2 binds to residues 293-393 of monomeric p53 in a ratio of one S100A2 dimer to one p53 monomer. *In vitro*, it also binds to tetrameric p53, but only with low affinity.[12-14]

It has been demonstrated that moderate and high levels of S100A2 expression in pancreatic cancer is a poor prognosis marker even after surgical resection. Patients displaying low levels of S100A2 in pancreatic cancer had a survival benefit post-surgery, even in the presence of lymph node metathesis.[15] S100A2 is upregulated in the aggressive and poor prognosis squamous subtype of PDAC and is a predictive biomarker of this disease

FULL PAPER

state.[15, 16, 17] It is found in high concentrations in the nucleus of cells, which is unique in the family of S100 proteins, and is associated with the regulation of cell cycling.[17] S100A2 modulates the tumour suppressor p53 by binding with its transactivation domain. In pancreatic cancer, over expression of S100A2 inhibits p53, preventing p53 tumour suppression, resulting in aberrant cancer cell proliferation.[18] Importantly, the inhibition of the S100 protein family binding to p53 has been the focus of drug discovery campaigns.

S100A2 is upregulated in the aggressive and poor prognosis squamous subtype of PDAC and is a predictive biomarker of this disease state.[19, 20] It is found in high concentrations in the nucleus of cells, which is unique in the family of S100 proteins, and is associated with the regulation of cell cycling.[21] S100A2 modulates the tumour suppressor p53 by binding with its transactivation domain. In pancreatic cancer, over expression of S100A2 inhibits p53, preventing p53 tumour suppression, resulting in aberrant cancer cell proliferation.[22] Importantly, the inhibition of the S100 protein

family binding to p53 has been the focus of drug discovery campaigns.

Results and Discussion

In silico analysis of the S100A2-p53 complex, using the Molecular Operating Environment (MOE) software system identified a surface pocket within S100A2, into which the p53 peptide showed good docking (Figure 1A). This "p53-groove", represents a protein-protein 'hot-spot area' potentially suitable for small molecule binding.[23]

Subsequent *in silico* screening of an in-house proprietary library of about 10,000 compounds identified sulfonamide **1**, which was predicted to block the interaction between S100A2 and p53 (Figure 1). MTT cytotoxicity evaluation revealed **1** to be a GI$_{50}$ 2.97 ± 0.03 μM inhibitor of the MiaPaCa-2 pancreatic cancer cell line. These data, in conjunction with the synthetic tractability of **1**, made it an interesting lead in the potential development of compounds active against pancreatic cancer. The development and cytotoxicity of focused analogue libraries of **1** is reported herein.
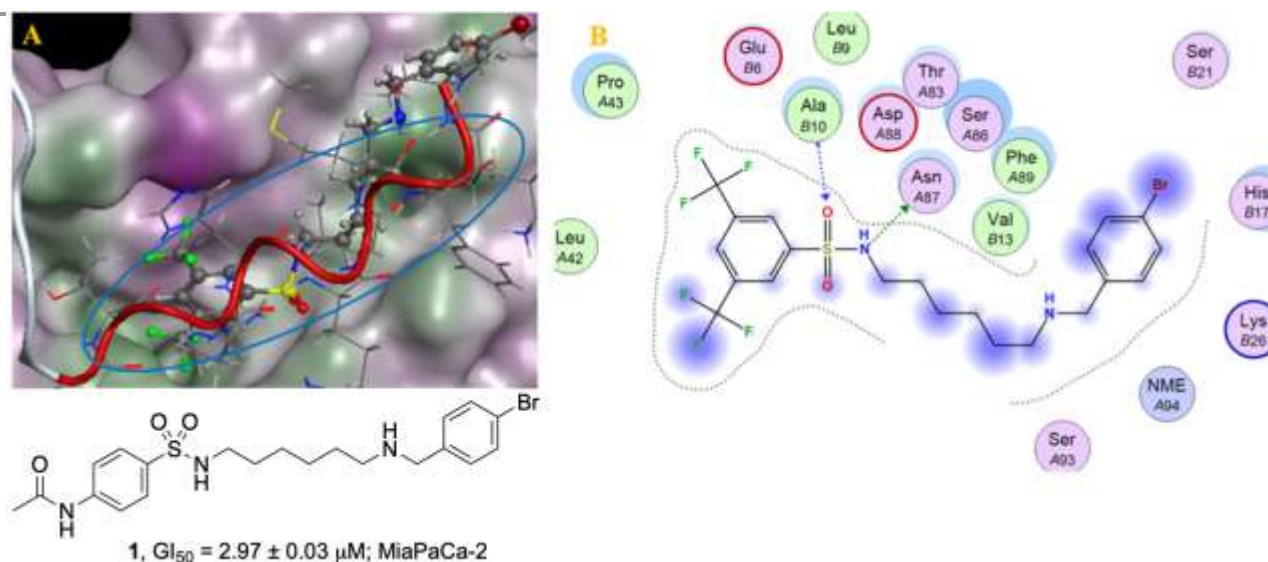

1, GI$_{50}$ = 2.97 ± 0.03 μM; MiaPaCa-2

Figure 1. A. Overlay of **1** with p53 peptide (red) predicted by MOE and p53 groove (highlighted by the blue oval); **1** is coloured by atom type; protein surface coloured: purple: hydrophilic area; green: hydrophobic area; **B.** The 2D MOE interaction plot of **1** depicting the adjacent amino acids. Key **1** interactions are shown (dashed lines) with S100A2. *A* and *B* in the amino acid identifiers refer to the 2 S100A2 chains in the homodimer sequence.

Library synthesis was envisaged from 3,5-bis(trifluoromethyl)benzene sulfonyl chloride (**2**), a selection of aminoalcohols (**3a-c**), and an aldehyde or amine (**4a** and/or **4b**) (Figure 2). This proposed modular approach was effected as shown in Scheme 1. *Library 1* was accessed on treatment of sulfonyl chloride (**2**) with 2-aminoethan-1-ol (**3a**) to give alcohol (**5**) followed by functional group interchange to install the mesylate (**6**). Nucleophilic displacement of the mesylate with selected amines afforded *Library 1* (**7**-**12**) with 25-72% yields (Experimental). *Library 1* possessed an ethyl linked diamine moiety (from **3a**).

2 **3a**, n = 0; **3b**; n =1, **3c**; n = 2

2
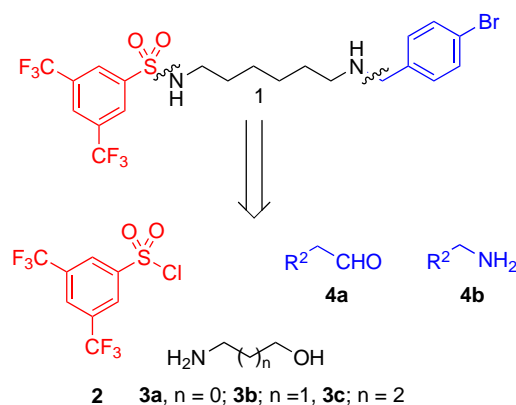
FULL PAPER

Figure 2. Chemical structure of Lead **1**; individual Library assembly fragments are coded by colour: sulfonyl chloride (**2**; **red**); aminoalcohol (**3a-c**; **black**) and aldehyde or amine (**4a,b**; **blue**).

Analysis of the *Library 1* MTT screening data at an initial 25 µM compound concentration (Supporting Information; Table S1) resulted in analogues **8**-**11** proceeding to full dose response evaluation (Table 1). Analogues **7** (4-BrPh) and **12** (4-CF$_3$) were insufficiently active to proceed to full dose response evaluation.
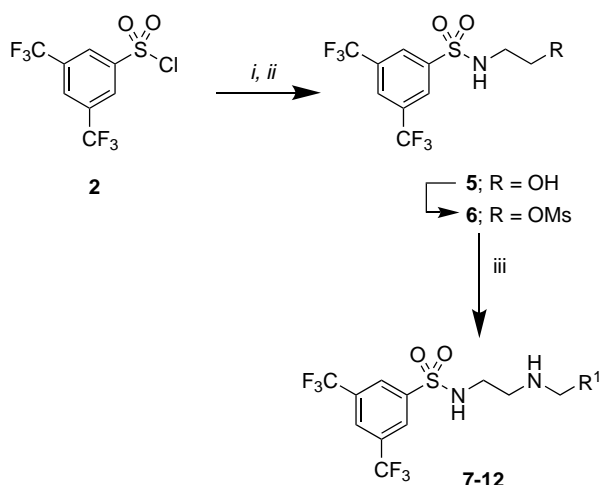
Scheme 1. Reagents and Conditions: (*i*) 2-aminoethanol (**3a**), NaHCO$_3$, H$_2$O, THF, RT, 4 h; (*ii*) CH$_3$SO$_2$Cl, pyridine, CH$_2$Cl$_2$, RT, 72 h; (*iii*) CH$_3$CN, pyridine, 80 ºC, 11 h. For details of R^1 see Tables 1 and 2.

Our human cancer cell line screening panel can be considered as comprising two separate cohorts, the first cohort (cohort-1) comprising: HT29 (colon), MCF-7 (breast), A2780 (ovarian), H460 (lung), A431 (skin), Du145 (prostate), BEC-2 and U87 (glioblastoma), SJ-G2 (neuroblastoma), and MCF10A (normal breast); with the second cohort (cohort-2) made up of the pancreatic cancer cell lines: MiaPaCa-2, BxPC-3, AsPC-1, Capan-2, PANC-1 and HPAC.
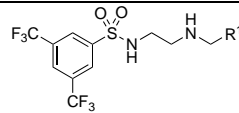
MTT screening of *Library 1* against cohort 1 cell lines revealed, for analogues **8**-**11** that proceeded to full dose response evaluation, a rank potency order of **10** (4-Ph-Ph) >> **9** (4-C(CH$_3$)$_3$Ph) > **11** (1-naphthyl) > **7** (3,4-di-OCH$_3$Ph). This suggests that the combination of steric bulk and an additional aromatic ring is beneficial to activity. The 1-naphthyl **11** adds steric constraints not present with **10**: and **9**, while sterically bulky, lacks the electron density associated with the second Ph moiety of **10**. The activity of **10** ranged from 1.4 (MCF-7 and U87) to 2.7 µM (HT29 and BE2-C) (Table 1).

Continued evaluation of *Library 1* in an expanded pancreatic cancer cell line panel was undertaken (Table 1). As with our standard cell line panel, the GI$_{50}$ values of analogues **8**-**11** were determined. Broad spectrum activity against pancreatic cancer cell lines was observed, with 4-Ph **10** clearly the most active with pancreatic cancer cell line GI$_{50}$ values

from 1.6 (BxPC-3) to 4.2 µM (PANC-1). However, **10** was also highly active against the normal cell line, MCF10A (GI$_{50}$ = 3.3 µM) indicating no cancer versus normal cell line selectivity in this model system. As **10** shows significant potency differences, at 5- to 10- fold greater against the pancreatic cancer cell line panel than **8** (3,4-di-OCH$_3$), **9** (4-C(CH$_3$)$_3$) or **12** (4-CF$_3$), the addition of the second phenyl moiety appears responsible for the enhanced cytotoxicity. This effect was not exclusively steric as both the 4-C(CH$_3$)$_3$ **9** and 1-naphthyl **11** were less active. In a similar manner the lone pair of electrons associated with the di-OCH$_3$ **7** did not contribute strongly to cytotoxicity (Table 1).

Molecular docking studies were performed using MOE for analogues **8**-**11** (*Library 1*) and showed very similar docking poses. The 3,5-*bis*-CF$_3$ moiety in these compounds aligned in the same direction. Additionally, the 3,4-diOCH$_3$Ph in compound **8**, 4-C(CH$_3$)$_3$ **9**, 4-Ph-Ph **10**, and 1-naphthyl **11** were oriented in a similar direction/position (Supporting Information; Figure S1). The bulky 4-Ph-Ph **10** extended the overall length of the molecule, which is thought to block the interaction between S100A2 and p53 more efficiently compared with the other compounds in *Library 1* (Figure 3A), whereas the 1-naphthyl **11** experiences a steric clash with the top right hand side of the p53 groove resulting in the decreased activity (Figure 3B).

Table 1. GI$_{50}$ (µM) determination of *Library 1* compounds **8**-**11** against various human cancer cell lines and the normal cell line MCF10A (normal breast). GI$_{50}$ is the compound concentration required to inhibit cell growth by 50% relative to an untreated control.

Cell Line	8 3,4-di-OCH$_3$Ph	9 4-C(CH$_3$)$_3$	10 4-Ph-Ph	11 1-naphthyl
R^1				
	GI$_{50}$ (µM)			
HT29[a]	13 ± 0.58	14 ± 0.58	2.7 ± 0.00	16 ± 1.0
MCF-7[b]	25 ± 1.5	13 ± 0.67	1.4 ± 0.19	18 ± 4.9
A2780[c]	14 ± 2.3	14 ± 1.0	2.6 ± 0.18	21 ± 2.0
A2780[c]	14 ± 2.3	14 ± 1.0	2.6 ± 0.18	21 ± 2.0
H460[d]	19 ± 3.2	14 ± 1.0	2.6 ± 0.15	-
A431[e]	25 ± 1.0	16 ± 0.67	2.4 ± 0.15	-
Du145[f]	30 ± 1.2	16 ± 0.33	2.5 ± 0.10	-
BE2-C[g]	23 ± 2.2	14 ± 0.58	2.7 ± 0.22	19 ± 0.67
U87[g]	25 ± 1.5	13 ± 0.67	1.4 ± 0.19	-
SJ-G2[h]	29 ± 0.58	14 ± 0.00	2.5 ± 0.18	-
MCF10A[i]	25 ± 2.4	14 ± 0.00	3.3 ± 0.25	22 ± 1.5
MiaPaCa-2[j]	29 ± 1.0	15 ± 0.33	2.7 ± 0.15	26 ± 2.2
BxPC-3[j]	20 ± 8.8	8.8 ± 3.2	1.6 ± 0.32	23 ± 6.5
AsPC-1[j]	20 ± 2.5	14 ± 1.2	2.8 ± 0.10	22 ± 0.58
Capan-2[j]	34 ± 2.6	13 ± 0.33	2.4 ± 0.40	21 ± 2.7
PANC-1[j]	34 ± 0.33	13 ± 0.58	4.2 ± 0.61	24 ± 3.9
HPAC[j]	16 ± 0.33	14 ± 0.58	2.8 ± 0.10	18 ± 0.00

[a] colon; [b] breast; [c] ovarian; [d] lung; [e] skin; [f] prostate; [g] glioblastoma; [h] neuroblastoma; [i] normal breast; [j] pancreas; '-' = not determined.
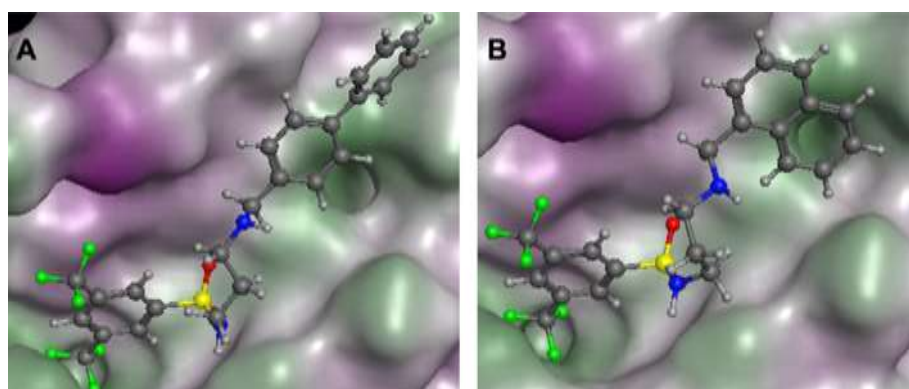
3

FULL PAPER

Figure 3. The docking poses of selected compounds in the S100A2 binding site: **A**. Compound **10**; **B**. Compound **11**. Compounds are coloured by atom type; Protein surface: purple, hydrophilic region; green, hydrophobic area.

Examination of the binding poses of *Library 1* analogues suggested that while the 3,5-bis(trifluoromethyl)benzene sulfonamide moiety engaged well with the p53 binding pocket, the terminal phenyl moiety failed to fully engage with the other side of the p53 binding groove. In turn this suggested that increasing the alkyl spacer from ethyl to propyl may have a positive effect on the observed cytotoxicity. To this end, *Library 2* was constructed using 3-aminopropan-1-ol (**3b**) to afford analogues **13**-**18** in 28-54% yields, and analogue **19** was produced commencing with 4-aminobutan-1-ol (**3c**) to examine the effect of further alkyl spacer elongation in 36% yield. These analogues were screened at 25 μM concentration with all analogues proceeding to full dose response evaluation (Table 2).

Uniformly, *Library 2* analogues were more active than their *Library 1* counterparts, supporting the hypothesis of alkyl spacer elongation. The *Library 2* compounds are all broad spectrum cytotoxic (cohort-1 cell lines) with the observed GI$_{50}$ values generally <4 μM potent excepting **14** (7 μM, A431). This high level of activity also extended to the cohort-2 analogues targeting pancreatic cancer. Activity against the (cohort-2) pancreatic cancer lines, GI$_{50}$ 1.4 (**15**, BxPC-3) to 18 μM (**14**, PANC-1). In all cases, simple halogen (**13** and **19**), alkyl (**15**), aromatic (**16** and **17**) and electron withdrawing (**18**) moieties afforded high levels of

anti-pancreatic cancer effects (Table 2). The increase in chain length resulted in a ca 10-fold potency increase for the 4-Br **13**, 5-fold increase for C(CH$_3$)$_3$ **14**, potency retention for 4-Ph-Ph **15**, a 10-fold potency for 1-naphthyl **17** and the 4-CF$_3$ **18** proceeded to GI$_{50}$ determination with GI$_{50}$ values of 1.4 (MCF-7) to 3.2 μM (PANC-1). All *Library 2* analogues displayed high levels of activity against the pancreatic cancer cell lines examined. These outcomes are consistent with the molecular modelling predictions.

The predicted docked poses of *Library 2* analogues align better with the terminus of the p53 groove (Figure 4A and B). In the docked pose of all *Library 2* compounds, better access to the p53 groove is noted, and this is consistent with the observed enhancement in cytotoxicity. This also supports the action of these compounds through inhibition of the S100A2-p53 interaction (but does not categorically prove). This increase in potency and engagement with the p53 groove is most evident for 1-naphthyl **17** and 4-CF$_3$ **18** with the extra flexibility afforded by the propyl chain allowing better access to the p53 groove, reflected in increased cytotoxicity. Further increase in alkyl spacer length (butyl *vs*. propyl with **13** *vs*. **19**) showed no additional increase in potency. This suggests that a propyl alkyl spacer is the optimal carbon chain length for inhibition of the S100A2-p53 interaction.

Table 2. GI$_{50}$ (μM) determination of *Library 2* compounds **13-19** against various human cancer cell lines and the normal cell line, MCF10A (normal breast). GI$_{50}$ is the compound concentration required to inhibit cell growth by 50% relative to an untreated control.

Cell Line							
	13	**14**	**15**	**16**	**17**	**18**	**19**
R^1	4-BrPh	3,4-diOCH$_3$Ph	4-C(CH$_3$)$_3$	4-Ph-Ph	1-naphthyl	4-CF$_3$	4-BrPh
n	1	1	1	1	1	1	2
	GI$_{50}$ (μM)						
HT29[a]	2.2±0.10	2.7±0.20	2.0±0.00	2.3±0.15	2.6±0.15	2.9±0.21	1.6±0.38
MCF-7[b]	1.9±0.05	1.9±0.00	2.1±0.15	1.7±0.35	1.4±0.17	1.4±0.20	1.5±0.19
A2780[c]	2.6±0.00	3.8±0.10	2.9±0.03	2.6±0.03	3.1±0.15	2.8±0.35	2.1±0.12
H460[d]	2.5±0.22	3.4±0.79	2.5±0.21	2.5±0.17	-	-	-
A431[e]	2.5±0.20	7.0±0.46	2.8±0.13	2.6±0.18	-	-	-
Du145[f]	2.6±0.17	4.0±0.32	2.7±0.20	2.7±0.09	-	-	-
BE2-C[g]	2.7±0.03	3.6±0.33	2.5±0.07	2.6±0.12	2.7±0.18	2.7±0.12	2.2±0.10

4

U87[g]	2.1±0.09	3.4±0.12	2.3±0.10	2.2±0.10	-	-	-
SJ-G2[h]	2.4±0.12	18±0.33	2.4±0.12	2.3±0.07	-	-	-
MCF10A[i]	3.1±0.19	5.3±0.62	3.2±0.15	2.8±0.12	3.2±0.03	3.3±0.09	3.2±0.07
MiaPaCa-2[j]	2.3±0.27	2.8±0.18	2.3±0.13	2.4±0.12	2.8±0.10	2.5±0.21	2.1±0.15
BxPC-3[j]	1.5±0.13	13±1.2	1.4±0.35	1.7±0.24	2.7±1.2	1.7±0.033	1.7±0.12
AsPC-1[j]	2.8±0.09	6.4±2.4	2.7±0.09	2.5±0.10	3.0±0.06	2.7±0.23	2.9±0.09
Capan-2[j]	2.0±0.31	15±1.3	2.1±0.10	2.2±0.06	2.7±0.27	2.0±0.21	1.9±0.27
PANC-1[j]	2.2±0.17	18±0.88	2.5±0.15	2.5±0.17	2.7±0.07	3.2±0.66	2.2±0.00
HPAC[j]	2.9±0.13	3.5±0.24	2.3±0.30	2.7±0.17	2.4±0.21	2.7±0.13	2.0±0.23

[a] colon; [b] breast; [c] ovarian; [d] lung; [e] skin; [f] prostate; [g] glioblastoma; [h] neuroblastoma; [i] normal breast; [j] pancreas; '-' = not determined.
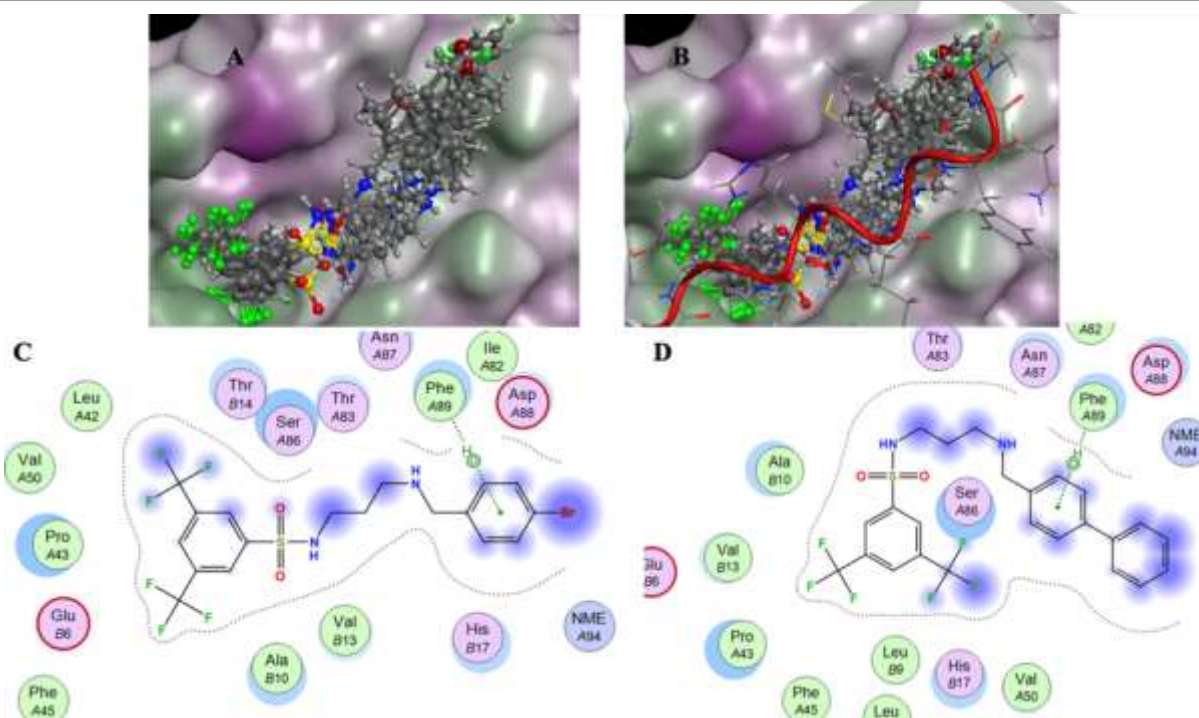

Figure 4. The highest scoring docking poses of selected *Library 2* compounds: **A.** superimposition of analogues **13**-**19**; **B.** as for A with the p53 peptide shown in red; compounds are coloured by atom type. Protein surface coloured: purple, hydrophilic region; green, hydrophobic region. **C**. The MOE 2D interaction plots depicting the compound adjacent amino acids, **C**. analogue **13** (4-Br); and **D**. As for **C** with analogue **16** (4-Ph). *A* and *B* in the amino acid identifiers refer to the 2 S100A2 chains in the homodimer

Compounds in *Library 2* also displayed similar docking poses (Figure 5) as compounds **8**-**11** in *Library 1*. The similar levels of inhibitory activity also can be explained via the MOE 2D interaction plot. Examination of Figure 5 highlights the similarity in binding poses for these compounds. Specifically, compounds **13-17** and **19** engage with the binding pocket through an arene-H interaction between the aryl ring and amino Phe*A*89 (e.g. Figure 4C, **13** (4-Br) and 4D, **16** (4-Ph); Supporting Information; Figure S2), and analogue **18** with the binding pocket via the sulfonamide nitrogen and amino Asn*A*87.
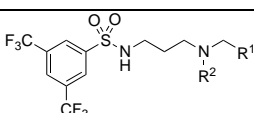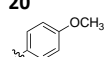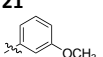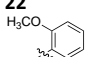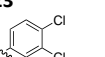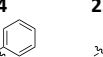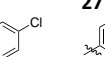
Library 2 analogues are more active than compounds in *Library 1* with the exception of compound **10**. The increased linker size for compounds in *Library 2* is hypothesised to be responsible for the increased activity. The increased linker length may increase the flexibility of the molecule and contribute to the enhanced binding between the molecules

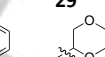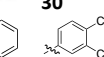and the binding pocket. This increased flexibility allowed enhanced interference in blocking the interaction between S100A2 and p53 peptide more effectively, leading to the improved activity for compounds with a three-carbon linker.

Having established the importance of the propyl linker, further investigation of the terminal phenyl ring substituents was undertaken with the synthesis of **20**-**30** from the corresponding aldehydes as per Scheme 1 in 39-71% yields (see Experimental). Within *Library 3* the effect of *N*-methylation of the parent phenyl analogue **24** was also explored. All *Library 3* analogues were sufficiently active at 25 μM concentration to proceed to full dose response evaluation (Table 3; Supporting Information, Table S3).

5

FULL PAPER

Table 3. GI$_{50}$ (μM) determination of *Library 3* compounds **20-30** against various human cancer cell lines and the normal cell line, MCF10 (normal breast). GI$_{50}$ is the compound concentration required to inhibit cell growth by 50% relative to an untreated control.

Cell Line	20	21	22	23	24	25	26	27	28	29	30
R^1	OCH$_3$	OCH$_3$	H$_3$CO	Cl Cl	phenyl	phenyl	Cl	Cl	Cl	O O	Cl CF$_3$
R^2	H	H	H	H	CH$_3$	H	H	H	H	H	H
GI$_{50}$ (μM)											
HT29[a]	2.9±0.25	10±3.5	12±1.2	4.7±0.95	>50	15±0.00	2.8±0.30	14±0.88	20±4.9	11±4.1	2.2±0.09
MCF-7[b]	2.5±0.03	2.4±0.09	2.6±0.21	2.4±0.24	16±1.9	3.0±0.03	2.4±0.13	2.6±0.12	8.8±3.2	3.5±0.63	2.5±0.17
A2780[c]	1.7±0.12	1.6±0.17	1.5±0.12	1.5±0.10	28±0.88	4.9±1.6	1.8±0.22	2.2±0.78	9.3±3.8	5.9±2.4	1.5±0.15
BE2-C[d]	2.8±0.12	4.5±1.1	3.6±0.26	2.9±0.19	28±2.3	12±0.73	2.9±0.03	6.9±2.1	15±5.5	8.6±2.4	2.8±0.00
MCF10A[e]	3.1±0.10	6.6±2.0	5.5±0.71	3.0±0.13	26±1.3	13±0.67	2.3±0.76	7.0±2.5	11±3.6	7.9±2.4	3.2±0.03
MiaPaCa-2[f]	2.5±0.10	3.4±0.57	3.1±0.36	2.7±0.10	33±3.0	11±0.29	2.8±0.18	4.4±1.3	11±4.0	7.4±2.4	2.6±0.22
BxPC-3[f]	1.3±0.22	1.7±0.64	1.7±0.60	1.4±0.21	39±5.9	13±0.58	1.6±0.12	3.8±1.3	11±4.6	7.8±3.3	1.2±0.35
AsPC-1[f]	2.8±0.21	3.8±0.57	4.6±0.37	2.8±0.03	51±2.1	13±1.5	3.0±0.06	5.9±2.5	13±5.0	9.6±3.4	2.9±0.15
Capan-2[f]	2.4±0.55	6.4±2.4	6.0±0.40	1.8±0.56	46±6.6	14±1.0	2.7±0.17	8.0±3.6	13±4.8	9.1±3.5	2.5±0.13
PANC-1[f]	11±0.60	10±1.6	12±0.58	5.6±1.30	>50	16±2.1	4.9±1.4	2.7±0.13	15±4.3	10±3.1	3.4±0.9
HPAC[f]	3.0±0.13	2.4±0.19	2.4±0.25	2.5±0.17	30±1.5	3.2±0.24	2.8±0.07	12±0.67	10±3.9	3.0±0.10	2.7±0.27

[a] colon; [b] breast; [c] ovarian; [d] glioblastoma; [e] normal breast; [f] pancreas.

The panel of cancer cell lines was reduced in the evaluation of *Library 3*, with analysis of the data presented in Table 3 against HT29, MCF-7, A2780 and BEC-2 cell lines being representative of our broad-spectrum panel. In this instance, the observed activity was generally similar to, or slightly lower than, observed with *Library 2*. There are key outliers to this data in particular the parent phenyl **25** with activity 5-fold lower, and a 10-fold potency reduction with N-CH$_3$ **24**. These data support, with **25**, the requirement for a phenyl substituent capable of accessing the upper area of the p53-groove; and the requirement for a H-bond donating capability with **24**. In the main, the nature of the phenyl substituent has little impact on the observed cytotoxicity if the analogue is capable of engaging with the p53-groove (Figure 5). Generally, *Library 3* compounds displayed good to high levels of cytotoxicity with GI$_{50}$ values ranging from 1.5 (**22**, **23** and **30**; A2780); to >50 μM (**24**; HT29).

Analogues **20**, **26** and **30** are all predicted to engage with S100A2 through an arene-H interaction between the benzene ring and Phe*A*89 respectively, and compound **23** binds with S100A2 through an interaction between the nitrogen atom of benzene- sulfonamide and Asn*A*87 (sidechain acceptor) (Figure 6). The introduction of the N-CH$_3$ moiety with **24** has a profound impact on the docked conformation in the p53-groove with the phenyl moiety twisting and the loss of a critical H-bond donor interaction (Figure 5C and D). This is reflected in the significant loss in cytotoxicity observed with a 5- to 10- fold decrease in potency recorded. The effect was most profound in the case of the panel of pancreatic cancer cell lines with all activities in the GI$_{50}$ range of >30 μM. This compares unfavourably with the corresponding free NH **25** which is 3- to 5- fold more active; and **24** is 15-fold less active than **30**, the most active analogue against the pancreatic cancer cell lines with GI$_{50}$ of 1.2 (BxPC-3) to 3.4 (PANC-1) μM. Of note it is known that the BxPC-3 cell line has high endogenous levels of S100A2 (Figure 7). Thus, the cytotoxicity response is in line with the predicted effect of blocking the S100A2-p53 interaction.
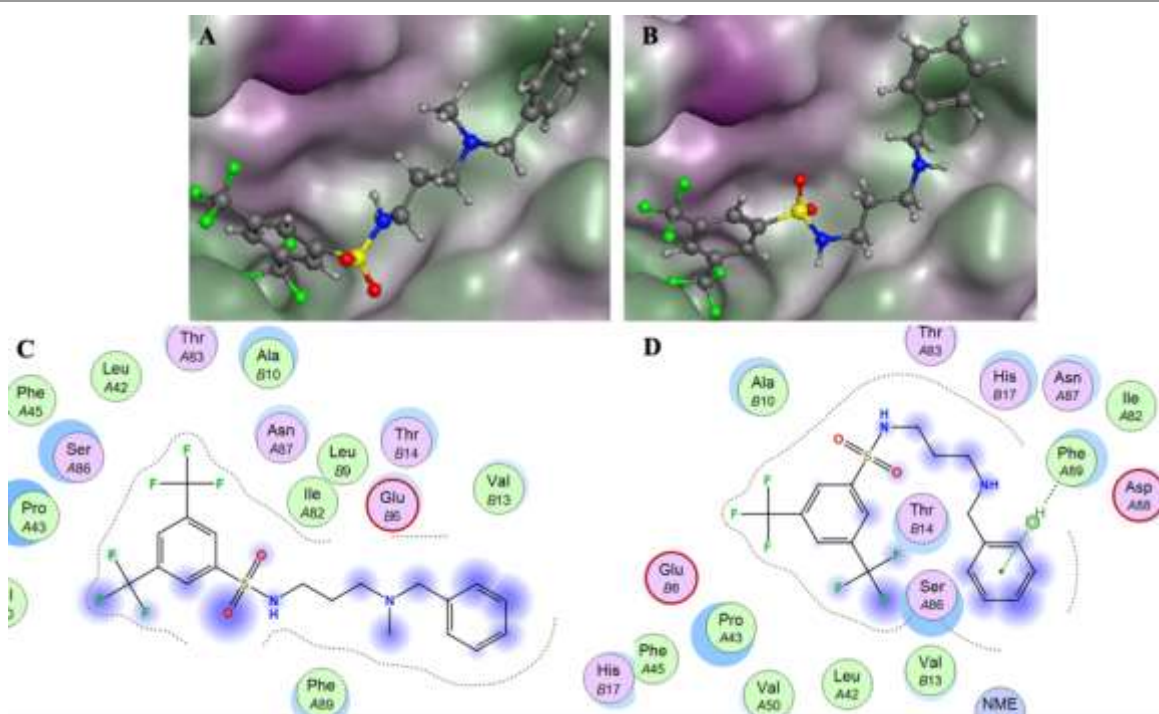
FULL PAPER

Figure 5. A. The best scoring binding pose of N- CH$_3$ **24**; **B.** best scoring binding pose of N- CH$_3$ **25**; Compounds coloured by atom type. Protein surface: purple, hydrophilic region; green, hydrophobic region. C. The MOE 2D interaction plots depicting the compound adjacent amino acids, with analogue **24**; **D**. As for **C** with analogue **25**. *A* and *B* in the amino acid identifiers refer to the 2 S100A2 chains in the homodimer
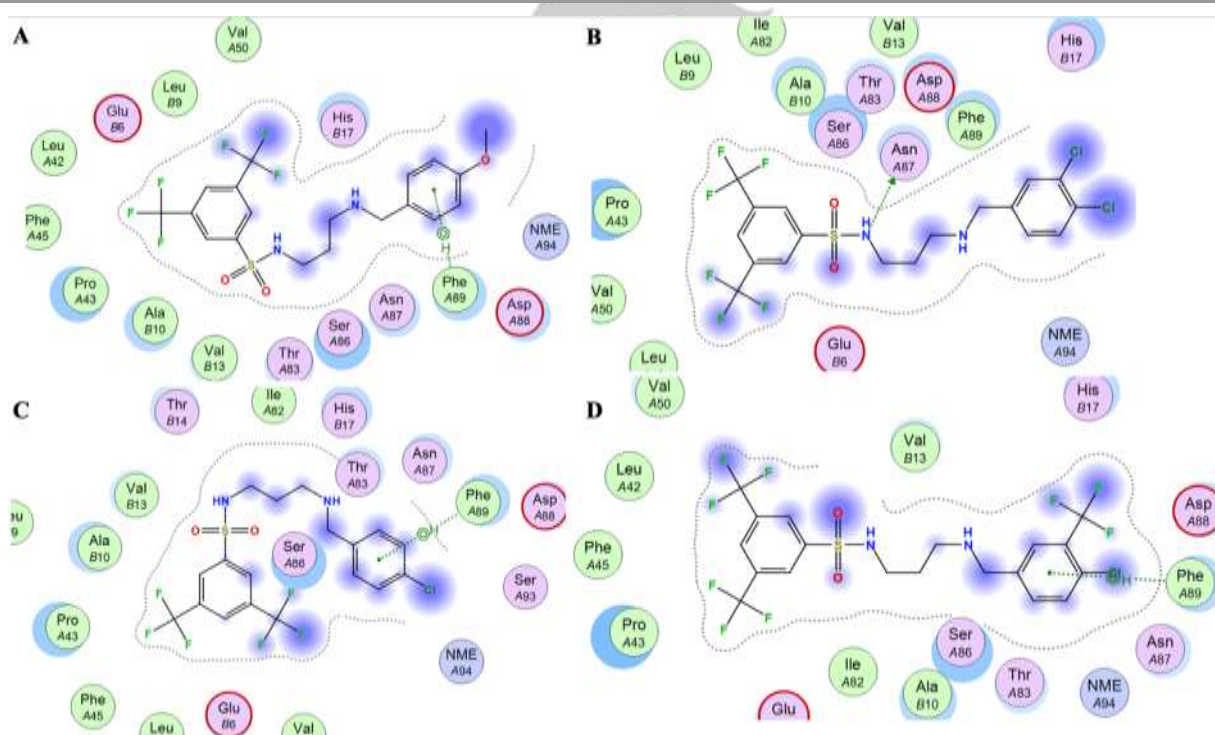

Figure 6. A. The MOE 2D interaction plots depicting the compound adjacent amino acids, with analogue **20**; **B.** As for C with analogue **23**; **C.** As for C with analogue **26**; **D.** As for C with analogue **30**. *A* and *B* in the amino acid identifiers refer to the 2 S100A2 chains in the homodimer.

7

FULL PAPER

Figure 7. High endogenous expression of S100A2 was observed in the PC cell line BxPC-3 via Western blot.

Conclusions

Virtual screening predicted sulfonamide **1** as an inhibitor of the S100A2-p53 protein-protein interaction. S100A2 is a validated pancreatic cancer drug target, and screening of **1** in the pancreatic cancer cell line, MiaPaCa-2, revealed it as a 2.97 µM potent cell growth inhibitor. The development of focused compound libraries (*Library 1, 2* and *3*) demonstrated that a propyl diamine linker gave rise to the highest level of both broad-spectrum cytotoxicity and pancreatic cancer cell line cytotoxicity. In total 15 human cell lines were evaluated. The introduction of a N-CH$_3$ substituent with **24** resulted in a 5- to 10-fold potency reduction relative to the free NH analogue **25**. Analysis of the cytotoxicity screening data revealed a poor correlation between the terminal phenyl substituent and cytotoxicity provided that the substituent could fully access the S100A2-p53 binding groove. As a consequence, it was noted that 4-substituted phenyl analogues were generally more active. In all instances there was good to excellent correlation between the predicted binding pose in the S100A2-p53 binding groove and the observed cytotoxicity. This was particularly evident upon examination of the cytotoxicity of *Library 2* and *Library 3* compounds against the six pancreatic cancer cell lines examined (MiaPaCa-2, BxPC-3, AsPC-1, Capan-2, HPAC and PANC-1). Combined, the data presented herein is consistent with the inhibition of the S100A2-p53 protein-protein interaction with an anti-pancreatic cancer drug target.

Experimental

Chemistry

General Methods

All reactions were performed using standard laboratory equipment and glassware. Solvents and reagents were purchased from Sigma Aldrich, Alfa Aesar or AK Scientific and used as received. Organic solvent extracts were dried over magnesium sulfate (MgSO$_4$), and dried under reduced pressure with either Büchi or Heidolph rotary evaporators. Melting points were recorded in open capillaries on a Büchi 565 Melting Point Apparatus. Where available, literature values are provided and appropriately referenced. Electrospray mass spectra were recorded using H$_2$O (with 1% formic acid, solvent A) and 90% MeCN in H$_2$O (with 1% formic acid, solvent B) as carrier solvents on an Agilent Technologies 1260 Infinity UPLC system with a 6120 Quadrupole LC/MS in electrospray ionization (ESI) positive and negative modes. TLC was performed on Merck silica gel 60 F254 precoated aluminium plates with a thickness of 0.2 mm. Nuclear magnetic resonance (NMR) spectroscopy was performed on a Bruker Avance III 400 MHz

(^{19}F, ^{1}H and ^{13}C NMR) at 400, 400 and 100 MHz respectively or a Bruker Avance III 600 MHz (^{1}H and ^{13}C NMR) spectra at 600 and 150 MHz respectively. All spectra were recorded in deuterated dimethyl sulfoxide (DMSO-d_6) obtained from Cambridge Isotope Laboratories Inc. Chemical shifts (d) were measured in parts per million (ppm) and referenced against the internal reference peaks. Coupling constants (*J*) were measured in Hertz (Hz). NMR assignments were determined through the interpretation of one- and two-dimensional spectra. Multiplicities are denoted as singlet (s), broad singlet (bs), doublet (d), doublet of doublets (dd), triplet (t), quartet (q), pentet (p), septet (sept) and multiplet (m). Peaks are listed in decreasing chemical shift in the following format: chemical shift integration (^{1}H), multiplicity (^{1}H), coupling constant (Hz).

N-[2-(4-Bromobenzylamino)-ethyl]-3,5-bis(trifluoromethyl)benzenesulfonamide hydrochloride **7**

To a solution of 2-aminoethanol (1.05 eq, 963 mg, 15.8 mmol) and NaHCO$_3$ (1.6 eq, 2.020 g, 24 mmol) in H$_2$O (40 mL) was gradually added a solution of 3,5-bis(trifluoromethyl)benzene sulfonyl chloride (1.0 eq, 4.689 g, 15 mmol) in THF (40 m L). The reaction mixture was allowed to stir for 5 h at RT, monitored by TLC (CH$_3$OH/DCM: 10:1, R$_f$: 0.78). After the reaction, THF was removed under vacuum. The residue was filtered and washed with water (500 mL) and hexanes (200 mL) to afford the desired product as a white solid. Yield: 4.121 g, 82%, m. p.: 88-90 ºC. ^{1}H NMR (400 MHz, DMSO-d_6) δ 8.48 (s, 1H), 8.40 (s, 2H), 8.10 (s, 1H), 4.72 (t, *J* = 5.3 Hz, 1H), 3.39 (q, 5.2 Hz, 2H), 2.90 (t, *J* = 5.8 Hz, 2H); ^{13}C NMR (101 MHz, DMSO-d_6) δ 143.7, 131.3 (q, *J* = 33.7 Hz, 2C), 127.3 (unresolved q, *J* = 3.5 Hz), 126.3 (unresolved sept, *J* = 3.6 Hz, 2C), 122.7 (q, *J* = 271.7 Hz, 2C), 59.8, 45.3; ^{19}F NMR (376 MHz, DMSO-d_6, CF$_3$CO$_2$H) δ -58.1; IR υ$_{max}$/cm^{-1}: 3289 (N-H), 3166 (O-H), 1276 (S=O), 1155 (S=O), 1129 (C-F), 1107 (C-N); LRMS (ESI$^+$) m/z: 338 [M +H].

To a solution of N-(2-hydroxyethyl)-3,5-bis(trifluoromethyl)-benzenesulfonamide (1 eq, 3.888 g, 11.5 mmol) and pyridine (2.5 eq, 2.275 g, 28.8 mmol) in CH$_2$Cl$_2$ (80 mL) was gradually added a solution of MsCl (2.2 eq, 2.885 g, 25.3 mmol) in CH$_2$Cl$_2$ (40 mL). The reaction mixture was allowed to stir for 4 h at RT, monitored by UPLC-MS analysis. After the reaction, the solvent was removed under vacuum. To the residue was added H$_2$O (100 mL), and the precipitate was collected and washed with water (300 mL) and hexanes (200 mL) by filtration and dried under reduced pressure to give the desired product as a white solid. Yield: 4.342 g, 91%, m. p.: 135-138 ºC. ^{1}H NMR (400 MHz, DMSO-d_6) δ 8.49 (s, 1H), 8.45 (t, *J* = 5.8 Hz, 1H), 8.39 (s, 2H), 4.15 (t, *J* = 5.1 Hz, 2H), 3.25 (q, 5.4 Hz, 2H), 3.11 (s, 3H); ^{13}C NMR (101 MHz, DMSO-d_6) δ 143.8, 131.9 (q, *J* = 33.6 Hz, 2C), 127.6 (unresolved quartet, *J* = 3.2 Hz, 2C), 127.0 (unresolved sept, *J* = 3.6 Hz), 122.7 (q, *J* = 271.7 Hz, 2C), 69.3, 42.2, 37.0; ^{19}F NMR (376 MHz, DMSO-d_6, CF$_3$CO$_2$H) δ -58.8; IR υ$_{max}$/cm^{-1}: 3289 (N-H), 1277 (S=O), 1160 (S=O), 1133 (C-F), 1112 (C-N); LRMS (ESI$^+$) m/z: 416 [M +H].

To a solution of 4-bromobenzylamine (2.0 eq, 371 mg, 2 mmol) and pyridine (1.0 eq, 80 mg, 1.0 mmol) in MeCN (30 mL) was added 2-(3,5-bis(trifluoromethyl)phenylsulfonamido)ethyl methanesulfonate (1.0 eq, 415 mg, 1.0 mmol). The reaction mixture was stirred for 11 h at 80 ºC, monitored by LC-MS analysis. Following the reaction, the mixture was filtered, then the filtrate was concentrated under reduced pressure. To the residue was added 2 mL acetone and 2 mL 10% HCl and dried under compressed air. The residue was washed with water (20 mL) and hexanes (20 mL) and then recrystallized using acetone (5 mL) and ether (10 mL) to give compound **7** as a hydrochloride salt, a white solid. Yield: 190 mg, 35%, m. p.: dec. >213 ºC. ^{1}H NMR (400 MHz, DMSO-d_6) δ 9.36 (s, 1H), 8.63 (s, 1H), 8.54 (s, 1H), 8.42 (s, 2H), 7.64 (d, *J* = 8.4 Hz, 2H), 7.49 (d, *J* = 8.4 Hz, 2H), 4.14 (s, 2H), 3.17 (s, 2H), 3.00 (s, 2H); ^{13}C NMR (101 MHz, DMSO-d_6) 142.5, 132.4 (2C), 131.5 (2C), 131.4 (q, *J* = 33.7, 2C), 131.2, 127.5 (unresolved quartet, *J* = 3.3 Hz), 126.9 (overlapping q, *J* = 3.4 Hz, 2C), 122.7 (q, *J* = 271.8 Hz, 2C), 122.4, 49.1, 45.8, 38.6; ^{19}F NMR (376 MHz, DMSO-d_6, CF$_3$CO$_2$H) δ -58.1; IR υ$_{max}$/cm^{-1}: 2989 (N-H), 1278 (S=O), 1163 (S=O), 1137 (C-F), 1095 (C-N), 681 (C-Br); LRMS (ESI$^+$) m/z: 505[M-HCl+H, ^{79}Br]/507 [M-HCl+H, ^{81}Br]; HRMS calculated for C$_{17}$H$_{16}$BrClF$_6$N$_2$O$_2$S [M-HCl+H, ^{79}Br]: 505.0014/[M-HCl+H, ^{81}Br]: 506.9991; found: 504.9942/506.9942.

N-[2-(3,4-Dimethoxybenzylamino)-ethyl]-3,5-bis(trifluoromethyl)benzene sulfonamide hydrochloride **8**

Synthesized using the general procedure as described for **23**, 2-(3,5-bis(trifluoromethyl)phenylsulfonamido)ethylmethanesulfonate (1.0 eq, 415 mg, 1.0 mmol) and 3,5-dimethoxybenzylamine (2.0 eq, 332 mg, 2.0 mmol) reacted (monitored by IPLC-MS analysis) to afford compound **8** as a hydrochloride salt, a white solid. Yield: 130 mg, 25%, m. p.: dec. >160 ºC. ^{1}H NMR (400 MHz, DMSO-d_6) δ 9.23 (s, 2H), 8.63 (s, 1H), 8.54 (s, 1H), 8.43 (s, 2H), 7.23 (d, *J* = 1.6 Hz, 1H), 7.02 - 6.96 (m, 2H), 4.07 (s, 2H), 3.77 (d, *J* = 4.3 Hz, 6H), 3.17 (s, 2H), 2.97 (s, 2H); ^{13}C NMR (101 MHz, DMSO-d_6) 149.3, 148.6, 142.5, 131.5 (q, *J* = 33.7 Hz, 2C), 127.5

8

FULL PAPER

(unresolved q, $J = 3.1$ Hz), 126.9 (overlapping q, $J = 3.5$ Hz, 2C), 123.8, 122.7, 122.6 (q, $J = 271.7$ Hz, 2C), 113.7, 115.5, 55.5 (2C), 49.8, 45.5, 38.7; ^{19}F NMR (376 MHz, DMSO-d_6, CF$_3$CO$_2$H) δ -58.1; IR υ_{max}/cm^{-1}: 2976 (N-H), 1277 (S=O), 1267 (C-O), 1162 (S=O), 1133 (C-F), 1107 (C-N), 1025 (C-O); LRMS (ESI$^+$) m/z: 487 [M-HCl+H]; HRMS calculated for C$_{19}$H$_{21}$ClF$_6$N$_2$O$_4$S [M-HCl+H]: 487.1121; found: 487.1048.

N-[2-(4-tert-Butylbenzylamino)-ethyl]-3,5-bis(trifluoromethyl)benzene sulfonamide hydrochloride 9

Synthesized using the general procedure as described for **7**, 2-(3,5-*bis*(trifluoromethyl)phenylsulfonamido)ethylmethanesulfonate (1.0 eq, 415 mg, 1.0 mmol) and 4-*tert*-butylbenzylamine (1.5 eq, 250 mg, 1.5 mmol) were reacted (monitored by UPLC-MS analysis) to afford compound **9** as a hydrochloride salt, a white solid. Yield: 150 mg, 29%, m. p.: dec. >186 ºC. ^{1}H NMR (400 MHz, DMSO-d_6) δ 9.23 (s, 2H), 8.64 (br s, 1H), 8.54 (s, 1H), 8.43 (s, 2H), 7.44 (s, 4H), 4.10 (s, 2H), 3.17 (t, $J = 6.4$ Hz, 2H), 3.00 (t, $J = 6.4$ Hz, 2H), 1.28 (s, 9H); ^{13}C NMR (101 MHz, DMSO-d_6) 151.5, 142.5, 131.5 (q, $J = 33.7$ Hz, 2C), 129.9 (2C), 128.9, 127.5 (unresolved q, $J = 3.3$ Hz), 126.9 (m, 2C), 125.4 (2C), 122.6 (q, $J = 271.8$ Hz, 2C), 49.6, 45.8, 38.7, 34.4, 31.0 (3C); ^{19}F NMR (376 MHz, DMSO-d_6, CF$_3$CO$_2$H) δ -58.1; IR υ_{max}/cm^{-1}: 2970 (N-H), 1279 (S=O), 1164 (S=O), 1128 (C-F), 1094 (C-N); LRMS (ESI$^+$) m/z: 483 [M-HCl+H]; HRMS calculated for C$_{21}$H$_{25}$ClF$_6$N$_2$O$_2$S [M-HCl+H]: 483.1534; found: 483.1463.

N-(2-(([1,1'-biphenyl]-4-ylmethyl)amino)ethyl)-3,5-bis(trifluoromethyl)benzene sulfonamide 10

Synthesized using the general procedure as described for **7**, 2-(3,5-*bis*(trifluoromethyl)phenylsulfonamido)ethylmethanesulfonate (1.0 eq, 415 mg, 1.0 mmol) and 4-phenylbenzylamine (1.5 eq, 273 mg, 1.5 mmol) were reacted (monitored by UPLC-MS analysis) to afford compound **10** as a white solid. Yield: 210 mg, 42%, m. p.: 129-131 ºC. ^{1}H NMR (400 MHz, DMSO-d_6) δ 8.48 (s, 1H), 8.39 (s, 2H), 7.64 (d, $J = 7.4$ Hz, 2H), 7.57 (d, $J = 8.1$ Hz, 2H), 7.45 (t, $J = 7.6$ Hz, 2H), 7.34 (dd, $J = 14.9$, 7.6 Hz, 3H), 3.65 (s, 2H), 2.97 (t, $J = 6.3$ Hz, 2H), 2.55 (t, $J = 6.1$ Hz, 2H). No signals of NH; ^{13}C NMR (101 MHz, DMSO-d_6) 143.6, 140.0, 139.2, 138.7, 131.4 (q, $J = 33.7$ Hz, 2C), 128.9 (2C), 128.6 (2C), 127.3, 127.2 (unresolved q, $J = 3.1$ Hz), 126.6 (2C), 126.4 (4C), 122.7 (q, $J = 271.7$ Hz, 2C), 52.0, 47.7, 42.5; ^{19}F NMR (376 MHz, DMSO-d_6, CF$_3$CO$_2$H) δ -58.1; IR υ_{max}/cm^{-1}: 2920 (N-H), 1277 (S=O), 1157 (S=O), 1117 (C-F), 1097 (C-N); LRMS (ESI$^+$) m/z: 503 [M-HCl+H]; HRMS calculated for C$_{23}$H$_{20}$F$_6$N$_2$O$_2$S [M-HCl+H]: 503.1220; found: 503.1150.

N-(2-((Naphthalen-1-ylmethyl)amino)ethyl)-3,5-bis(trifluoromethyl)benzene sulfonamide hydrochloride 11

Synthesized using general procedure as described for **7**, 2-(3,5-*bis*(trifluoromethyl)-phenylsulfonamido)ethylmethane sulfonate (1.0 eq, 415 mg, 1.0 mmol) and 1-naphthylmethylamine (1.5 eq, 240 mg, 1.5 mmol) were reacted (monitored by UPLC-MS analysis) to afford the desired compound **11** as a hydrochloride salt, an off-white solid. Yield: 220 mg, 43%, m. p.: dec. >235 ºC. ^{1}H NMR (400 MHz, DMSO-d_6) δ 9.26 (s, 2H), 8.66 (s, 1H), 8.55 (s, 1H), 8.43 (s, 2H), 8.23 (d, $J = 8.1$ Hz, 1H), 8.02 (d, $J = 7.9$ Hz, 2H), 7.74 (d, $J = 7.0$ Hz, 1H), 7.67 − 7.55 (m, 3H), 4.67 (s, 2H), 3.22 (s, 4H); ^{13}C NMR (101 MHz, DMSO-d_6) 142.5, 133.3, 131.5 (q, $J = 33.7$ Hz, 2C), 131.1, 129.7, 129.1, 128.7, 128.0, 127.5 (unresolved q, $J = 2.9$ Hz, 2C), 126.9 (unresolved sept, $J = 3.6$ Hz), 126.8, 126.3, 125.3, 123.8, 122.6 (q, $J = 271.8$ Hz, 2C), 46.8, 46.5, 38.7; ^{19}F NMR (376 MHz, DMSO-d_6, CF$_3$CO$_2$H) δ -58.1; IR υ_{max}/cm^{-1}: 2855 (N-H), 1278 (S=O), 1164 (S=O), 1107.0 (C-F), 1097 (C-N); LRMS (ESI$^+$) m/z: 477 [M-HCl+H]; HRMS calculated for C$_{24}$H$_{23}$ClF$_6$N$_2$O$_2$S [M-HCl+H]: 477.1065; found: 477.0993.

3,5-Bis(trifluoromethyl)-N-[2-(4-trifluoromethylbenzylamino)-ethyl]-benzene sulfonamide hydrochloride 12

Synthesized using the general procedure as described for **7**, 2-(3,5-*bis*(trifluoromethyl)phenylsulfonamido)ethylmethanesulfonate (1.0 eq, 415 mg, 1.0 mmol) and 4-(trifluoromethyl)benzylamine (2 eq, 352 mg, 2 mmol) were reacted (monitored by UPLC-MS analysis) to afford compound **12** as a hydrochloride salt, a white solid. Yield: 381 mg, 72%, m. p.: dec. >212 ºC. ^{1}H NMR (400 MHz, DMSO-d_6) δ 9.46 (s, 2H), 8.63 (s, 1H), 8.53 (s, 1H), 8.42 (s, 2H), 7.81 (d, $J = 8.3$ Hz, 2H), 7.76 (d, $J = 8.2$ Hz, 2H), 4.25 (s, 2H), 3.19 (t, $J = 6.3$ Hz, 2H), 3.02 (t, $J = 6.3$ Hz, 2H); ^{13}C NMR (101 MHz, DMSO-d_6) 142.5, 136.5, 131.5 (q, $J = 33.7$ Hz, 2C), 131.0 (2C), 129.4 (q, $J = 31.7$ Hz), 127.5 (unresolved q, $J = 3.1$ Hz, 2C), 126.8 (unresolved sept, $J = 3.4$ Hz), 125.4 (q, $J = 3.7$ Hz, 2C), 124.1 (q, $J = 270.5$ Hz), 122.6 (q, $J = 271.8$ Hz, 2C), 49.2, 46.0, 38.6; ^{19}F NMR (376 MHz, DMSO-d_6, CF$_3$CO$_2$H) δ -58.8, -59.0; IR υ_{max}/cm^{-1}: 2982 (N-H), 1279 (S=O), 1162 (S=O), 1125 (C-F), 1096 (C-N); LRMS (ESI$^+$) m/z: 495 [M-HCl+H]; HRMS calculated for C$_{18}$H$_{16}$ClF$_9$N$_2$O$_2$S [M-HCl+H]: 495.0785; found: 495.0710.

N-(3-((4-bromobenzyl)amino)propyl)-3,5-bis(trifluoromethyl)benzene sulfonamide hydrochloride 13

Synthesized using the general procedure as described for **7**, 3-aminopropanol (1.05 eq, 0.788 mg, 10.5 mmol) and 3,5-*bis*(trifluoromethyl)benzene-1-sulfonyl chloride (1.0 eq, 3.121 g, 10 mmol) were

reacted (monitored by TLC CH$_3$OH/DCM: 10:1, R$_f$: 0.80) to afford the desired product as a white solid. Yield: 2.811 g, 80%, m. p.: 95-97 ºC. ^{1}H NMR (400 MHz, DMSO-d_6) δ 8.50 (s, 1H), 8.37 (s, 2H), 7.99 (s, 1H), 4.40 (s, 1H), 3.35 (d, $J = 6.2$ Hz, 2H), 2.88 (t, $J = 7.2$ Hz, 2H), 1.55 − 1.49 (m, 2H); ^{13}C NMR (101 MHz, DMSO-d_6) δ 143.4, 131.5 (q, $J = 33.7$ Hz, 2C), 127.2 (unresolved q, $J = 3.5$ Hz, 2C), 126.5 (unresolved sept, $J = 3.5$ Hz), 122.8 (q, $J = 271.7$ Hz, 2C), 57.8, 39.9, 32.4; ^{19}F NMR (376 MHz, DMSO-d_6, CF$_3$CO$_2$H) δ -58.9; IR υ_{max}/cm^{-1}: 3483 (N-H), 3120 (O-H), 1276 (S=O), 1157 (S=O), 1135 (C-F), 1107 (C-N); LRMS (ESI$^+$) m/z: 352 [M+H].

3-(3,5-*bis*(trifluoromethyl)phenylsulfonamido)propyl methane sulfonate was obtained from N-(3-hydroxypropyl)-3,5-*bis*(trifluoromethyl)-benzenesulfonamide (1 eq, 4.436 g, 12.64 mmol) and MsCl (2.0 eq, 2.886 g, 25.28 mmol) (monitored by UPLC-MS analysis) as a white solid. Yield: 4.887 g, 90%, m. p.: 121-124 ºC. ^{1}H NMR (400 MHz, DMSO-d_6) δ 8.51 (s, 1H), 8.38 (s, 2H), 8.16 (t, $J = 5.8$ Hz, 1H), 4.19 (t, $J = 6.2$ Hz, 2H), 3.14 (s, 3H), 2.93 (dd, $J = 12.9$, 6.7 Hz, 2H), 1.80 (p, $J = 6.6$ Hz, 2H); ^{13}C NMR (101 MHz, DMSO-d_6) δ 143.0, 131.5 (q, $J = 33.6$ Hz, 2C), 127.2 (q, $J = 3.3$ Hz, 2C), 126.7 (unresolved sept, $J = 3.5$ Hz), 122.6 (q, $J = 271.7$ Hz, 2C), 67.5, 38.8, 36.5, 28.8; ^{19}F NMR (376 MHz, DMSO-d_6, CF$_3$CO$_2$H) δ -58.6; IR υ_{max}/cm^{-1}: 3263 (N-H), 1277 (S=O), 1164 (S=O), 1131 (C-F), 1106 (C-N); LRMS (ESI$^+$) m/z: 430 [M+H].

Following this, 4-bromobenzylamine (2.0 eq, 0.37 g, 2.0 mmol) and 3-(3,5-*bis*(trifluoromethyl)phenylsulfonamido)propylmethane sulfonate (1.0 eq, 429 mg, 1 mmol) were reacted (monitored by UPLC-MS analysis) to afford compound 7-**29** as a hydrochloride salt, a white solid. Yield: 301 mg, 54%, m. p.: dec. >235 ºC. ^{1}H NMR (400 MHz, DMSO-d_6) δ 9.21 (br s, 2H), 8.52 (s, 1H), 8.33 (br s, 1H), 8.39 (s, 2H), 7.64 (d, $J = 8.4$ Hz, 2H), 7.49 (d, $J = 8.4$ Hz, 2H), 4.09 (s, 2H), 2.90 (t, $J = 7.0$ Hz, 4H), 1.8 −1.78 (m, 2H); ^{13}C NMR (101 MHz, DMSO-d_6) 143.0, 132.3 (2C), 131.5 (2C), 131.5 (q, $J = 33.6$ Hz, 2C), 131.4, 127.3 (unresolved q, $J = 3.3$ Hz), 126.6 (overlapping q, $J = 3.4$ Hz, 2C), 122.6 (q, $J = 271.8$ Hz, 2C), 122.3, 49.2, 44.0, 39.9, 26.0; ^{19}F NMR (376 MHz, DMSO-d_6, CF$_3$CO$_2$H) δ -58.1; IR υ_{max}/cm^{-1}: 2941 (N-H), 1275 (S=O), 1158 (S=O), 1134 (C-F), 1088 (C-N), 680 (C-Br); LRMS (ESI$^+$) m/z: 519 [M-HCl+H, ^{79}Br]/521 [M-HCl+H, ^{81}Br]; HRMS calculated for C$_{18}$H$_{18}$ClF$_6$N$_2$O$_2$S [M-HCl+H, ^{79}Br]: 519.0171/[M-HCl+H, ^{81}Br]: 521.0148; found: 519.0098/521.0098.

N-[3-(3,4-Dimethoxybenzylamino)-propyl]-3,5-bis(trifluoromethyl)benzene sulfonamide hydrochloride 14

Synthesized using the general procedure as described for **13**, 3,5-dimethoxybenzylamine (2.0 eq, 330 mg, 2 mmol) and 3-(3,5-*bis*(trifluoromethyl)phenylsulfonamido)propylmethane sulfonate (1.0 eq, 429 mg, 1 mmol) were reacted (monitored by UPLC-MS analysis) to afford compound **14** as a hydrochloride salt, a white solid. Yield: 270 mg, 50%, m. p.: dec. >207 ºC. ^{1}H NMR (400 MHz, DMSO-d_6) δ 9.12 (s, 2H), 8.52 (s, 1H), 8.40 (s, 2H), 8.33 (br s, 1H), 7.24 (d, $J = 1.7$ Hz, 1H), 7.03 − 7.00 (m, 2H), 4.03 (s, 2H), 3.78 (s, 3H), 3.76 (s, 3H), 2.90 (s, 4H), 1.86 − 1.79 (m, 2H); ^{13}C NMR (101 MHz, DMSO-d_6) 149.2, 148.6, 143.1, 131.5 (q, $J = 33.6$ Hz, 2C), 127.3 (unresolved q, $J = 3.1$ Hz), 126.6 (overlapping q, $J = 3.5$ Hz, 2C), 124.0, 122.7 (q, $J = 272.1$Hz, 2C), 122.6, 113.8, 111.5, 55.6, 55.5, 49.9, 43.7, 39.9, 26.0; ^{19}F NMR (376 MHz, DMSO-d_6, CF$_3$CO$_2$H) δ -58.1; IR υ_{max}/cm^{-1}: 2934 (N-H), 1275 (S=O), 1267 (C-O), 1159 (S=O), 1133 (C-F), 1085 (C-N), 1027 (C-O); LRMS (ESI$^+$) m/z: 501 [M-HCl+H]; HRMS calculated for C$_{20}$H$_{23}$ClF$_6$N$_2$O$_4$S [M-HCl+H]: 501.1275; found: 501.1204.

N-[3-(4-tert-Butylbenzylamino)-propyl]-3,5-bis(trifluoromethyl)benzene sulfonamide hydrochloride 15

Synthesized using the general procedure as described for **13**, 4-*tert*-butylbenzylamine (2.0 eq, 330 mg, 2.0 mmol) and 3-(3,5-*bis*(trifluoromethyl)phenylsulfonamido)propylmethane sulfonate (1.0 eq, 429 mg, 1 mmol) were reacted (monitored by UPLC-MS analysis) to afford compound **15** as a hydrochloride salt, a white solid. Yield: 231 g, 43%, m. p.: dec. >241 ºC. ^{1}H NMR (400 MHz, DMSO-d_6) δ 9.12 (br s, 2H), 8.52 (s, 1H), 8.34 (br s, 1H), 8.40 (s, 2H), 7.45 (s, 4H), 4.05 (s, 2H), 2.93 − 2.89 (m, 4H), 1.86 − 1.79 (m, 2H), 1.28 (s, 9H); ^{13}C NMR (101 MHz, DMSO-d_6) 151.5, 143.1, 131.5 (q, $J = 33.6$ Hz, 2C), 129.9 (2C), 129.1, 127.3 (unresolved q, $J = 3.2$ Hz), 126.7 (overlapping q, $J = 3.4$ Hz, 2C), 125.4 (2C), 122.7 (q, $J = 271.7$ Hz, 2C), 49.7, 44.1, 39.9, 34.4, 31.0 (3C), 26.0; ^{19}F NMR (376 MHz, DMSO-d_6, CF$_3$CO$_2$H) δ -58.1; IR υ_{max}/cm^{-1}: 2934.0 (N-H), 1280.1 (S=O), 1164.9 (S=O), 1136.9 (C-F), 1082.1 (C-N); LRMS (ESI$^+$) m/z: 497.2 [M-HCl+H]; HRMS calculated for C$_{22}$H$_{27}$ClF$_6$N$_2$O$_2$S [M-HCl+H]: 497.1691; found: 497.1619.

N-(3-(([1,1'-biphenyl]-4-ylmethyl)amino)propyl)-3,5-bis(trifluoromethyl)benzene sulfonamide hydrochloride 16

Synthesized using the general procedure for **13**, 4-phenylbenzylamine (2.0 eq, 369 mg, 2.0 mmol) and 3-(3,5-*bis*(trifluoromethyl)phenylsulfonamido)propyl-methanesulfonate (1.0 eq, 429 mg, 1.0 mmol) were reacted (monitored by UPLC-MS analysis) to afford compound **16** as a hydrochloride salt, a white solid. Yield: 160 mg, 29%, m. p.: dec. >239 ºC. ^{1}H NMR (400 MHz, DMSO-d_6) δ 9.23 (s, 2H),

9

FULL PAPER

8.52 (s, 1H), 8.37 (br s, 1H), 8.40 (s, 2H), 7.74 – 7.68 (m, 4H), 7.63 (d, J = 8.2 Hz, 2H), 7.49 (t, J = 7.6 Hz, 2H), 7.39 (t, J = 7.3 Hz, 1H), 4.15 (s, 2H), 2.97 – 2.90 (m, 4H), 1.89 –1.82 (m, 2H); ^{13}C NMR (101 MHz, DMSO-d$_6$) 143.1, 140.6, 139.4, 131.4 (q, J = 33.6, 2C), 131.1, 130.7 (2C), 129.0 (2C), 127.8, 127.3 (unresolved q, J = 3.2 Hz), 126.8 (2C), 126.7 (2C), 126.6 (overlapping q, J = 3.4 Hz, 2C), 122.6 (q, J = 271.7 Hz, 2C), 49.6, 44.1, 39.9, 26.0; ^{19}F NMR (376 MHz, DMSO-d$_6$, CF$_3$CO$_2$H) δ -58.2; IR υ$_{max}$/cm^{-1}: 2940 (N-H), 1281 (S=O), 1158 (S=O), 1128 (C-F), 1092 (C-N); LRMS (ESI$^+$) m/z: 517 [M-HCl+H]; HRMS calculated for C$_{24}$H$_{23}$ClF$_6$N$_2$O$_2$S [M-HCl+H]: 517.1377; found: 517.1306.

N-(3-((naphthalen-1-ylmethyl)amino)propyl)-3,5-bis(trifluoromethyl)benzene sulfonamide hydrochloride **17**

Synthesized using the general procedure as described for **13**, 1-naphthylmethylamine (1.5 eq, 240 mg, 1.5 mmol) and 3-(3,5-bis(trifluoromethyl)phenylsulfonamido)propylmethane sulfonate (1.0 eq, 429 mg, 1.0 mmol) were reacted (monitored by LC-MS analysis) to afford compound **17** as a hydrochloride salt, a white solid. Yield: 201m g, 38%, m. p.: dec. >242 ºC. ^{1}H NMR (400 MHz, DMSO-d$_6$) δ 9.15 (s, 2H), 8.53 (s, 1H), 8.41 (s, 2H), 8.36 (br s, 1H), 8.23 (d, J = 8.2 Hz, 1H), 8.02 (d, J = 8.4 Hz, 2H), 7.76 (d, J = 6.7 Hz, 1H), 7.68 – 7.56 (m, 3H), 4.63 (s, 2H), 3.10 (t, J =7.7 Hz, 2H), 2.92 (t, J = 6.7 Hz, 2H), 1.92 – 1.85 (m, 2H); ^{13}C NMR (101 MHz, DMSO-d$_6$) 143.1, 133.3, 131.5 (q, J = 33.6 Hz, 2C), 131.1, 129.6, 129.1, 128.7, 128.1, 127.3 (unresolved q, J = 2.9 Hz), 126.8, 126.6 (unresolved sept, J = 3.3 Hz), 126.3, 125.3, 123.8, 122.7 (q, J = 271.7 Hz, 2C), 46.9, 44.9, 39.9, 26.0; ^{19}F NMR (376 MHz, DMSO-d$_6$, CF$_3$CO$_2$H) δ -58.6; IR υ$_{max}$/cm^{-1}: 2842 (N-H), 1279 (S=O), 1159 (S=O), 1131 (C-F), 1117 (C-N); LRMS (ESI$^+$) m/z: 491.2 [M-HCl+H]; HRMS calculated for C$_{21}$H$_{19}$ClF$_6$N$_2$O$_2$S [M-HCl+H]: 491.1221; found: 491.1105.

3,5-Bis-trifluoromethyl-N-[3-(4-trifluoromethylbenzylamino)-propyl]-benzene sulfonamide hydrochloride **18**

Synthesized using the general procedure as described for **13**, 4-(trifluoromethyl)benzylamine (2.5 eq, 440 mg, 2.5 mmol) and 3-(3,5-bis(trifluoromethyl)phenylsulfonamido propylmethane sulfonate (1.0 eq, 429 mg, 1.0 mmol) were reacted (monitored by UPLC-MS analysis) to afford compound **18** as a hydrochloride salt, a white solid. Yield: 150 mg, 28%, m. p.: dec. >207 ºC. ^{1}H NMR (400 MHz, DMSO-d$_6$) δ 9.33 (s, 2H), 8.51 (s, 1H), 8.39 (s, 2H), 8.33 (s, 1H),7.82 (d, J = 8.4 Hz, 2H), 7.77 (d, J = 8.3 Hz, 2H), 4.22 (s, 2H), 2.95 – 2.89 (m, 4H), 1.87 – 1.80 (m, 2H); ^{13}C NMR (101 MHz, DMSO-d$_6$) 143.1, 136.7, 131.5 (q, J = 33.7 Hz, 2C), 131.0 (2C), 129.3 (q, J = 31.6 Hz), 127.3 (unresolved q, J = 3.2 Hz, 2C), 126.6 (unresolved sept, J = 3.5 Hz), 125.4 (q, J = 3.8 Hz, 2C), 124.1 (q, J = 270.5 Hz), 122.6 (q, J = 271.7 Hz, 2C), 49.3, 44.3, 39.9, 26.0; ^{19}F NMR (376 MHz, DMSO-d$_6$, CF$_3$CO$_2$H) δ -57.8, -58.0; IR υ$_{max}$/cm^{-1}: 2981 (N-H), 1275 (S=O), 1159 (S=O), 1133 (C-F), 1068 (C-N); LRMS (ESI$^+$) m/z: 509 [M-HCl +H]; HRMS calculated for C$_{19}$H$_{18}$ClF$_9$N$_2$O$_2$S M-HCl+H]: 509.0942; found: 509.0867.

N-[4-(4-Bromo-benzylamino)-butyl]-3,5-bis(trifluoromethyl)benzenesulfonamide hydrochloride **19**

A solution of 4-bromobenzaldehyde (0.5 eq, 912 mg, 5.0 mmol) and butane-1,4-diamine (1.0 eq, 881 mg, 1.0 mmol) in methanol (40 mL) was stirred for 20 h at RT. Then NaBH$_4$ was added at 0 ºC and the reaction mixture was stirred for another 1 h (monitored by UPLC-MS analysis). The crude was washed with 1 M NaOH 60 mL and extracted with DCM (3 x 30 mL). The organic layer was dried with anhydrous MgSO$_4$ and concentrated under reduced pressure. The residue was triturated with methanol (3 x 10 mL) and cold ether (3 x 20 mL) to afford the desired product as a white solid. Yield: 520 mg, 41%, purity > 90% by NMR and LC-MS analysis. The product used directly in the next step without purification.

A solution of N^1-(4-bromobenzyl)-butane-1,4-diamine (1.0 eq, 130 mg, 0.5 mmol) in methanol (10 mL) was added 3,5-bis(trifluoromethyl)benzenesulfonyl chloride (1.1. eq, 169 mg, 0.55 mmol) slowly over 1 h at 0 ºC, then stirred for another 2 h (monitored by UPLC-MS analysis). The crude was washed using aqueous NH$_4$Cl (30 mL). The organic was concentrated. The residue was dissolved using 2 mL acetone and 4 mL 10% HCl was added. The mixture was filtered and triturated three times using cold ether (3 x 10 mL) to afford the desired compound **19** as a hydrochloride salt, a white solid. Yield: 100 mg, 36%, m. p.: 202-206 ºC. ^{1}H NMR (400 MHz, DMSO-d$_6$) δ 9.10 (s, 2H), 8.50 (s, 1H), 8.38 (s, 2H), 8.19 (t, J = 5.8 Hz, 1H), 7.64 (d, J = 8.4 Hz, 2H), 7.48 (d, J = 8.4 Hz, 2H), 4.08 (t, J = 16.8 Hz, 2H), 2.86 – 2.78 (m, 4H), 1.69-1.61 (m, 2H), 1.49 – 1.41 (m, 2H); ^{13}C NMR (101 MHz, DMSO-d$_6$) 143.2, 132.4 (2C), 131.6 (2C), 131.5 (q, J = 33.7 Hz, 2C), 131.4, 127.3 (unresolved q, J = 3.2 Hz), 126.6 (unresolved sept, J = 3.5 Hz), 122.7 (q, J = 271.8 Hz, 2C), 122.4, 49.2, 46.0, 42.0, 26.3, 22.6; ^{19}F NMR (376 MHz, DMSO-d$_6$, CF$_3$CO$_2$H) δ -58.5; IR υ$_{max}$/cm^{-1}: 2972.8 (N-H), 1279.8 (S=O), 1167.5 (S=O), 1135.2 (C-F), 1108.9 (C-N), 682.3 (C-Br); LRMS (ESI$^+$) m/z: 533 [M-HCl+H,

^{79}Br]/535 [M-HCl+H, ^{81}Br]; HRMS calculated for C$_{23}$H$_{29}$ClF$_3$N$_5$O$_5$S [M-HCl+H, ^{79}Br]: 533.0326/[M-HCl+H, ^{81}Br]: 535.0304; found: 533.0255/535.0255.

N-[3-(4-Methoxybenzylamino)-propyl]-3,5-bis(trifluoromethyl)benzenesulfonamide hydrochloride **20**

Synthesized using the general procedure as described for **13**, 4-methoxy-benzylamine (2.5 eq, 340 mg, 2.5 mmol) and 3-(3,5-bis(trifluoromethyl)phenylsulfonamido)propylmethane sulfonate (1.0 eq, 429 mg, 1 mmol) were reacted (monitored by UPLC-MS analysis) to afford compound **20** as a hydrochloride salt, a white solid. Yield: 310 mg, 61%, m. p.: 224-227 ºC. ^{1}H NMR (400 MHz, DMSO-d$_6$) δ 9.08 (s, 2H), 8.51 (s, 1H), 8.39 (s, 2H), 8.35 (s, 1H), 7.45 (d, J = 8.7 Hz, 2H), 6.97 (d, J = 8.7 Hz, 2H), 4.03 (s, 2H), 3.76 (s, 3H), 2.88 (dd, J = 14.0, 7.1 Hz, 4H), 1.85 – 1.78 (m, 2H); ^{13}C NMR (101 MHz, DMSO-d$_6$) 159.7, 143.1, 131.7 (2C), 131.4 (q, J = 33.7 Hz, 2C), 127.3 (unresolved q, J = 3.2 Hz, 2C), 126.6 (unresolved sept, J = 3.5 Hz), 123.8, 122.6 (q, J = 271.8 Hz, 2C), 113.9 (2C), 55.2, 49.4, 43.7, 39.9, 24.9; ^{19}F NMR (376 MHz, DMSO-d$_6$, CF$_3$CO$_2$H) δ -58.0; IR υ$_{max}$/cm^{-1}: 2942 (N-H), 1280 (S=O), 1249 (C-O), 1164 (S=O), 1133 (C-F), 1076 (C-N); LRMS (ESI$^+$) m/z: 471 [M-HCl+H]; HRMS calculated for C$_{19}$H$_{21}$ClF$_6$N$_2$O$_3$S [M-HCl+H]: 471.1166; found: 471.1099.

N-[3-(3-Methoxybenzylamino)-propyl]-3,5-bis(trifluoromethyl)benzenesulfonamide hydrochloride **21**

Synthesized using the general procedure as described for **13**, 3-methoxy-benzylamine (2.5 eq, 340 mg, 2.5 mmol) and 3-(3,5-bis(trifluoromethyl)phenyl-sulfonamido)propylmethane sulfonate (1.0 eq, 429 mg, 1.0 mmol) were reacted (monitored by UPLC-MS analysis) to afford compound **21** as a hydrochloride salt, a white solid. Yield: 270 mg, 53%, m. p.: 213-216 ºC. ^{1}H NMR (400 MHz, DMSO-d$_6$) δ 9.27 (s, 2H), 8.50 (s, 1H), 8.40 (s, 2H), 8.18 (s, 1H), 7.32 (t, J = 7.9 Hz, 1H), 7.21 (s, 1H), 7.08 (d, J = 7.3 Hz, 1H), 6.96 (d, J = 7.5 Hz, 1H), 4.06 (s, 2H), 3.77 (s, 3H), 2.90 (t, J = 6.7 Hz, 4H), 1.89 – 1.79 (m, 2H); ^{13}C NMR (101 MHz, DMSO-d$_6$) 159.3, 143.1, 133.5, 131.4 (q, J = 33.6 Hz, 2C), 129.7, 127.3 (unresolved q, J = 3.1 Hz, 2C), 126.6 (unresolved sept, J = 3.4 Hz), 122.6 (q, J = 271.8 Hz, 2C), 122.0, 115.5, 114.5, 55.2, 49.9, 44.0, 39.9, 26.0; ^{19}F NMR (376 MHz, DMSO-d$_6$, CF$_3$CO$_2$H) δ -58.1; IR υ$_{max}$/cm^{-1}: 2940 (N-H), 1273 (S=O), 1265 (C-O), 1164 (S=O), 1138 (C-F), 1093 (C-N); LRMS (ESI$^+$) m/z: 471 [M-HCl+H] ; HRMS calculated for C$_{19}$H$_{21}$ClF$_6$N$_2$O$_3$S [M-HCl+H]: 471.1168; found: 471.1099.

N-[3-(2-Methoxybenzylamino)-propyl]-3,5-bis(trifluoromethyl)benzene sulfonamide hydrochloride **22**

Synthesized using the general procedure as described for **13**, 2-methoxy-benzylamine (2.5 eq, 340m g, 2.5 mmol) and 3-(3,5-bis(trifluoromethyl)phenylsulfonamido)propylmethane sulfonate (1.0 eq, 429 mg, 1.0 mmol) were reacted (monitored by UPLC-MS analysis) to afford compound **22** as a hydrochloride salt, a white solid. Yield: 270 mg, 53%, m. p.: 208-211 ºC^{1}H NMR (400 MHz, DMSO-d$_6$) δ 8.93 (s br, 2H), 8.52 (s, 1H), 8.40 (s, 2H), 8.35 (s br , 1H), 7.45 – 7.39 (m, 2H), 7.09 (d, J = 8.0 Hz, 1H), 6.99 (td, J = 7.5, 0.8 Hz, 1H), 4.05 (s, 2H), 3.83 (s, 3H), 2.90 (t, J = 6.8 Hz, 4H), 1.87 – 1.79 (m, 2H); ^{13}C NMR (101 MHz, DMSO-d$_6$) 157.5, 143.1, 131.5, 131.5 (q, J = 33.6 Hz, 2C), 130.8, 127.3 (unresolved q, J = 3.1 Hz, 2C), 126.6 (unresolved sept, J = 3.5 Hz), 122.6 (q, J = 271.8 Hz, 2C), 120.3, 119.7, 111.1, 55.6, 44.9, 44.1, 39.9, 25.8; ^{19}F NMR (376 MHz, DMSO-d$_6$, CF$_3$CO$_2$H) δ -58.1; IR υ$_{max}$/cm^{-1}: 2963 (N-H), 1281 (S=O), 1251 (C-O) 1181 (S=O), 1134 (C-F), 1112 (C-N); LRMS (ESI$^+$) m/z: 471 [M-HCl+H]; HRMS calculated for C$_{19}$H$_{21}$ClF$_6$N$_2$O$_3$S [M-HCl+H]: 471.1169; found: 471.1099.

N-[3-(3,4-Dichlorobenzylamino)-propyl]-3,5-bis(trifluoromethyl)benzene sulfonamide hydrochloride **23**

Synthesized using the general procedure as described for **13**, 3,4-dichloro-benzylamine (2.5 eq, 441 mg, 2.5 mmol) and 3-(3,5-bis(trifluoromethyl)phenyl-sulfonamido)propylmethane sulfonate (1.0 eq, 429 mg, 1.0 mmol) were reacted (monitored by UPLC-MS analysis) to afford compound **23** as a hydrochloride salt, a white solid. Yield: 341 mg, 62%, m. p.: 231-234 ºC. ^{1}H NMR (400 MHz, DMSO-d$_6$) δ 9.27 (s, 2H), 8.52 (s, 1H), 8.39 (s, 2H), 8.32 (s, 1H), 7.87 (d, J = 1.9 Hz, 1H), 7.72 (d, J = 8.3 Hz, 1H), 7.53 (dd, J = 8.3, 2.0 Hz, 1H), 4.13 (s, 2H), 2.91 (dd, J = 11.9, 6.1 Hz, 4H), 1.85 – 1.78 (m, 2H); ^{13}C NMR (101 MHz, DMSO-d$_6$) 143.0, 133.1, 132.3, 131.6, 131.4 (q, J = 33.6 Hz, 2C), 131.1, 130.7, 130.6, 127.3 (unresolved q, J = 3.1 Hz, 2C), 126.6 (unresolved sept, J = 3.5 Hz), 122.6 (q, J = 271.7 Hz, 2C), 48.6, 44.1, 39.9, 26.0; ^{19}F NMR (376 MHz, DMSO-d$_6$, CF$_3$CO$_2$H) δ -58.0; IR υ$_{max}$/cm^{-1}: 2930 (N-H), 1275 (S=O), 1159 (S=O), 1134 (C-F), 1088 (C-N), 681 (C-Cl); LRMS (ESI$^+$) m/z: 509 [M-HCl+H, ^{35}Cl]/510 [M-HCl+H, ^{37}Cl]; HRMS calculated for C$_{18}$H$_{17}$Cl$_3$F$_6$N$_2$O$_2$S [M-HCl+H, ^{35}Cl]: 509.0282/[M-HCl+H, ^{37}Cl]: 511.0252; found: 509.0214.

N-[3-(Benzylmethylamino)-propyl]-3,5-bis(trifluoromethyl)benzenesulfonamide hydrochloride **24**

FULL PAPER

Synthesized using the general procedure as described for **13**, benzyl-methyl-amine (2.5 eq, 300 mg, 2.5 mmol) and 3-(3,5-*bis*(trifluoromethyl)phenyl-sulfonamido)propylmethane sulfonate (1.0 eq, 429 mg, 1.0 mmol) were reacted (monitored by UPLC-MS analysis) to afford compound **24** as a hydrochloride salt, a white solid. Yield: 0.35 g, 71%, m. p.: 124-127 ºC. ^{1}H NMR (400 MHz, DMSO-d$_6$) δ 10.53 (s, 1H), 8.52 (s, 1H), 8.39 (s, 2H), 8.33 (t, J = 5.9 Hz, 1H), 7.57 (dd, J = 6.0, 2.9 Hz, 2H), 7.46 – 7.45 (m, 3H), 4.35 (dd, J = 13.0, 4.2 Hz, 1H), 4.21 (dd, J = 12.9, 5.9 Hz, 1H), 3.15 – 3.08 (m, 1H), 3.02 – 2.95 (m, 1H), 2.87 (q, J = 6.5 Hz, 2H), 2.60 (d, J = 4.6 Hz, 3H), 1.94 – 1.87 (m, 2H); ^{13}C NMR (101 MHz, DMSO-d$_6$) 142.9, 131.6, 131.3, 131.4 (q, J = 33.4 Hz, 2C), 130.0, 129.4, 128.7 (2C), 127.3 (unresolved q, J = 3.1 Hz, 2C), 126.6 (unresolved sept, J = 3.4 Hz), 122.6 (q, J = 271.7 Hz, 2C), 58.2, 52.2, 39.9, 38.6, 23.8; ^{19}F NMR (376 MHz, DMSO-d$_6$, CF$_3$CO$_2$H) δ -58.0; IR υ$_{max}$/cm^{-1}: 2948 (N-H), 1282 (S=O), 1160 (S=O), 1132 (C-F), 1080 (C-N); LRMS (ESI$^+$) m/z: 455 [M-HCl+H]; HRMS calculated for C$_{19}$H$_{21}$ClF$_6$N$_2$O$_2$S [M-HCl+H]: 455.1221; found: 455.1150.

N-(3-Benzylaminopropyl)-3,5-bis(trifluoromethyl)benzene sulfonamide hydrochloride 25

Synthesized using the general procedure as described for **13**, benzylamine (2.5 eq, 274 mg, 2.5 mmol) and 3-(3,5-*bis*(trifluoromethyl)phenylsulfonamido)propylmethane sulfonate (1.0 eq, 429 mg, 1.0 mmol) were reacted (monitored by UPLC-MS analysis) to afford compound **25** as a hydrochloride salt, a white solid. Yield: 300 mg, 63%, m. p.: 214-217 ºC. ^{1}H NMR (400 MHz, DMSO-d$_6$) δ 9.20 (s, 2H), 8.52 (s, 1H), 8.39 (s, 2H), 8.34 (s, 1H), 7.53 (dd, J = 7.5, 2.0 Hz, 2H), 7.45 – 7.40 (m, 3H), 4.10 (s, 2H), 2.91 (dd, J = 13.4, 8.0 Hz, 4H), 1.87 – 1.79 (m, 2H); ^{13}C NMR (101 MHz, DMSO-d$_6$) 143.1, 132.0, 131.5 (q, J = 33.6, 2C), 130.1 (2C), 128.9, 128.6 (2C), 127.3 (unresolved q, J = 3.1 Hz, 2C), 126.6 (unresolved sept, J = 3.4 Hz), 122.6 (q, J = 271.7 Hz, 2C), 50.0, 44.1, 39.9, 25.9; ^{19}F NMR (376 MHz, DMSO-d$_6$, CF$_3$CO$_2$H) δ -58.0; IR υ$_{max}$/cm^{-1}: 2927 (N-H), 1278 (S=O), 1167 (S=O), 1128 (C-F), 1107 (C-N); LRMS (ESI$^+$) m/z: 441 [M-HCl+H] ; HRMS calculated for C$_{18}$H$_{19}$ClF$_6$N$_2$O$_2$S [M-HCl+H]: 441.1059; found: 441.0993.

N-[3-(4-Chlorobenzylamino)-propyl]-3,5-bis(trifluoromethyl)benzene sulfonamide hydrochloride 26

Synthesized using the general procedure as described for **13**, 4-chloro-benzylamine (2.5 eq, 349 mg, 2.5 mmol) and 3-(3,5-*bis*(trifluoromethyl)phenyl-sulfonamido)propylmethane sulfonate (1.0 eq, 429 mg, 1.0 mmol) were reacted (monitored by UPLC-MS analysis) to afford compound **26** as a hydrochloride salt, a white solid. Yield: 201 mg, 39%, m. p.: 228-231 ºC. ^{1}H NMR (400 MHz, DMSO-d$_6$) δ 9.23 (s, 2H), 8.51 (s, 1H), 8.39 (s, 2H), 8.33 (s, 1H), 7.57 – 7.55 (m, 2H), 7.52 – 7.49 (m, 2H), 4.11 (s, 2H), 2.89 (d, J = 6.1 Hz, 4H), 1.85 – 1.78 (m, 2H); ^{13}C NMR (101 MHz, DMSO-d$_6$) 143.1, 133.7, 132.1 (2C), 131.8 (q, J = 33.7 Hz, 2C), 131.0, 128.6 (2C), 127.3 (unresolved q, J = 3.2 Hz, 2C), 126.6 (unresolved sept, J = 3.4 Hz), 122.6 (q, J = 271.7 Hz, 2C), 49.1, 44.0, 39.9, 26.0; ^{19}F NMR (376 MHz, DMSO-d$_6$, CF$_3$CO$_2$H) δ -58.0; IR υ$_{max}$/cm^{-1}: 2937 (N-H), 1276 (S=O), 1159 (S=O), 1135 (C-F), 1088 (C-N), 681 (C-Cl); LRMS (ESI$^+$) m/z: 475 [M-HCl+H, ^{35}Cl]/477 [M-HCl+H, ^{37}Cl]; HRMS calculated for C$_{18}$H$_{18}$Cl$_2$F$_6$N$_2$O$_2$S [M-HCl+H, ^{35}Cl]: 475.0673/[M-HCl+H, ^{37}Cl]: 477.0641; found: 475.0603.

N-[3-(3-Chlorobenzylamino)-propyl]-3,5-bis(trifluoromethyl)benzenesulfonamide hydrochloride 27

Synthesized using the general procedure as described for **13**, 3-chloro-benzylamine (2.5 eq, 350 mg, 2.5 mmol) and 3-(3,5-*bis*(trifluoromethyl)phenyl-sulfonamido)propylmethane sulfonate (1.0 eq, 429 mg, 1.0 mmol) were reacted (monitored by UPLC-MS analysis) to afford compound **27** as a hydrochloride salt, a white solid. Yield: 230 mg, 45%, m. p.: 227-230 ºC. ^{1}H NMR (400 MHz, DMSO-d$_6$) δ 9.24 (s, 2H), 8.51 (s, 1H), 8.39 (s, 2H), 8.34 (s, 1H), 7.67 (s, 1H), 7.51 – 7.44 (m, 3H), 4.12 (s, 2H), 2.91 (dd, J = 13.2, 6.6 Hz, 4H), 1.86 – 1.79 (m, 2H); ^{13}C NMR (101 MHz, DMSO-d$_6$) 143.1, 134.4, 133.1, 131.5 (q, J = 33.6 Hz, 2C), 130.4, 130.0, 128.9, 128.8, 127.3 (unresolved quartet, J = 3.1 Hz, 2C), 126.6 (unresolved sept, J = 3.3 Hz), 122.6 (q, J = 271.7 Hz, 2C), 49.3, 44.2, 39.9, 26.0; ^{19}F NMR (376 MHz, DMSO-d$_6$, CF$_3$CO$_2$H) δ -58.0; IR υ$_{max}$/cm^{-1}: 2937 (N-H), 1281 (S=O), 1159 (S=O), 1134 (C-F), 1084 (C-N), 682 (C-Cl); LRMS (ESI$^+$) m/z: 475 [M-HCl+H, ^{35}Cl]/477 [M-HCl+H, ^{37}Cl]; HRMS calculated for C$_{18}$H$_{18}$Cl$_2$F$_6$N$_2$O$_2$S [M-HCl+H, ^{35}Cl]: 475.0673/[M-HCl+H, ^{37}Cl]: 477.0641; found: 475.0603.

N-[3-(2-Chlorobenzylamino)-propyl]-3,5-bis(trifluoromethyl)benzene sulfonamide hydrochloride 28

Synthesized using the general procedure as described for **13**, 2-chloro-benzylamine (2.5 eq, 350 mg, 2.5 mmol) and 3-(3,5-*bis*(trifluoromethyl)phenyl-sulfonamido)propylmethane sulfonate (1.0 eq, 429 mg, 1.0 mmol) were reacted (monitored by UPLC-MS analysis) to afford compound **28** as a hydrochloride salt, a white solid. Yield: 228 mg, 45%, m. p.: 237-240 ºC. ^{1}H NMR (400 MHz, DMSO-d$_6$) δ 9.29 (s br, 2H), 8.52 (s, 1H), 8.40 (s, 2H), 8.35 (s br, 1H), 7.72 (dd, J = 6.8, 2.5 Hz, 1H), 7.55 (dd, J = 7.3, 2.0 Hz, 1H), 7.48 – 7.42 (m, 2H), 4.22 (s, 2H), 2.99 (t, J =

7.5 Hz, 2H), 2.92 (t, J = 6.8 Hz, 2H), 1.89 – 1.82 (m, 2H); ^{13}C NMR (101 MHz, DMSO-d$_6$) 143.1, 133.6, 132.0, 131.5 (q, J = 33.6 Hz, 2C), 130.8, 129.8, 129.6, 127.5, 127.3 (unresolved q, J = 3.1 Hz, 2C), 126.6 (unresolved sept, J = 3.3 Hz), 122.6 (q, J = 271.7 Hz, 2C), 47.0, 44.5, 39.9, 25.9; ^{19}F NMR (376 MHz, DMSO-d$_6$, CF$_3$CO$_2$H) δ -58.1; IR υ$_{max}$/cm^{-1}: 2921 (N-H), 1276 (S=O), 1159 (S=O), 1134 (C-F), 1087 (C-N), 681 (C-Cl); LRMS (ESI$^+$) m/z: 475 [M-HCl+H]; HRMS calculated for C$_{18}$H$_{18}$Cl$_2$F$_6$N$_2$O$_2$S [M-HCl+H]: 475.0673/[M-HCl+H, ^{37}Cl]: 477.0641; found: 475.0603.

N-{3-[(2,3-Dihydrobenzo[1,4]dioxin-2-ylmethyl)-amino]-propyl}-3,5-bis(trifluoromethyl)benzene sulfonamide hydrochloride 29

Synthesized using the general procedure as described for **13**, 2-aminomethyl-1,4-benzodioxane (2.5 eq, 411 mg, 2.5 mmol) and 3-(3,5-*bis*(trifluoromethyl)phenylsulfonamido)propylmethane sulfonate (1.0 eq, 429 mg, 1.0 mmol) were reacted (monitored by UPLC-MS analysis) to afford compound **29** as a hydrochloride salt, an off-white solid. Yield: 281 mg, 53%, m. p.: dec. >220 ºC. ^{1}H NMR (400 MHz, DMSO-d$_6$) δ 9.33 (s br, 1H), 9.11 (s br, 1H), 8.52 (s, 1H), 8.40 (s, 2H), 8.35 (t, J = 5.5 Hz, 1H), 6.91 – 6.87 (m, 4H), 4.61 (t, J = 7.3 Hz, 1H), 4.36 (dd, J = 11.6, 2.2 Hz, 1H), 4.05 (dd, J = 11.7, 6.8 Hz, 1H), 3.28 (s, 1H), 3.19 – 3.14 (m, 1H), 3.01 (d, J = 6.2 Hz, 2H), 2.92 (dd, J = 11.1, 5.8 Hz, 2H), 1.88 – 1.81 (m, 2H); ^{13}C NMR (101 MHz, DMSO-d$_6$) 143.1, 142.7, 141.9, 131.5 (q, J = 33.7, 2C), 127.3 (unresolved q, J = 3.0 Hz, 2C), 126.6 (unresolved sept, J = 3.7 Hz), 122.6 (q, J = 271.7 Hz, 2C), 121.72, 121.68, 117.4, 117.1, 69.1, 64.8, 46.4, 45.0, 39.8, 25.9; ^{19}F NMR (376 MHz, *DMSO-d$_6$, CF$_3$CO$_2$H*) δ -58.0; IR υ$_{max}$/cm^{-1}: 2970 (N-H), 1276 (S=O), 1167 (S=O), 1134 (C-F), 1108 (C-O), 1080 (C-N); LRMS (ESI$^+$) m/z: 499 [M-HCl+H]; HRMS calculated for C$_{20}$H$_{21}$ClF$_6$N$_2$O$_4$S [M-HCl+H]: 499.1114; found: 499.1048.

N-[3-(4-Chloro-3-trifluoromethylbenzylamino)-propyl]-3,5-bis(trifluoromethyl)benzenesulfonamide hydrochloride 30

Synthesized using the general procedure as described for **13**, 4-chloro-3-trifluoromethylbenzylamine (2.5 eq, 520m g, 2.5 mmol) and 3-(3,5-*bis*(trifluoro-methyl)phenylsulfonamido)propylmethane sulfonate (1.0 eq, 429 mg, 1.0 mmol) were reacted (monitored by UPLC-MS analysis) to afford compound **30** as a hydrochloride salt, an off-white solid. Yield: 309 mg, 53%, m. p.: dec. >230 ºC. ^{1}H NMR (400 MHz, DMSO-d$_6$) δ 9.25 (s br, 2H), 8.52 (s, 1H), 8.39 (s, 2H), 8.32 (s br, 1H), 8.10 (s, 1H), 7.87 – 7.80 (m, 2H), 4.21 (s, 2H), 2.95-2.89 (m, 4H), 1.85 – 1.78 (m, 2H); ^{13}C NMR (101 MHz, DMSO-d$_6$) 143.0, 136.1, 132.1, 131.9, 131.5 (q, J = 33.7, 2C), 131.3 (unresolved q, J = 1.8 Hz), 129.9 (q, J = 5.1 Hz), 127.3 (unresolved q, J = 3.3 Hz, 2C), 126.63 (q, J = 30.8 Hz), 126.6 (unresolved sept, J = 3.5 Hz), 122.7 (q, J = 271.5 Hz), 122.6 (q, J = 271.7 Hz, 2C), 48.7, 44.2, 39.8, 26.1; ^{19}F NMR (376 MHz, DMSO-d$_6$, CF$_3$CO$_2$H) δ -58.0, 58.1; IR υ$_{max}$/cm^{-1}: 2960 (N-H), 1275 (S=O), 1176 (S=O), 1133 (C-F), 1089 (C-N), 680 (C-Cl); LRMS (ESI$^+$) m/z: 543 [M-HCl+H, ^{35}Cl]/545 [M-HCl+H, ^{37}Cl]; HRMS calculated for C$_{19}$H$_{17}$Cl$_2$F$_9$N$_2$O$_2$S [M-HCl+H, ^{35}Cl]: 543.0546/[M-HCl+H, ^{37}Cl]: 545.0516; found: 543.0477.

Biology

Cell culture and stock solutions

Stock solutions were prepared as follows and stored at -20 °C: drugs were stored as 40 mM solutions in DMSO. All cell lines were cultured in a humidified atmosphere 5% CO$_2$ at 37 ºC. The cancer cell lines were maintained in Dulbecco's modified Eagle's medium (DMEM) (Trace Biosciences, Australia) supplemented with 10% foetal bovine serum, 10 mM sodium bicarbonate, penicillin (100 IU/mL), streptomycin (100 μg/mL), and glutamine (4 mM). The non-cancer MCF10A cell line was cultured in DMEM:F12 (1:1) cell culture media, 5% heat inactivated horse serum, supplemented with penicillin (50 IU/mL), streptomycin (50 μg/mL), 20mM Hepes, L-glutamine (2mM), epidermal growth factor (20ng/mL), hydrocortisone (500ng/mL), cholera toxin (100ng/mL), and insulin (10 μg/mL).

In vitro growth inhibition MTT assay

Cells in logarithmic growth were transferred to 96-well plates. Cytotoxicity was determined by plating cells in duplicate in 100 μL medium at a density of 2500-4000 cells/well. On day 0, (24 h after plating) when the cells were in logarithmic growth 100 μL medium with or without the test agent was added to each well. After 72 h drug exposure growth inhibitory effects were evaluated using the MTT (3-[4,5-dimethylthiazol-2-yl]-2,5-diphenyl- tetrazolium bromide) assay and absorbance read at 540 nm. Percentage growth inhibition was determined at a fixed drug concentration of 25 μM. A value of 100% is indicative of complete cell growth inhibition. Those analogues showing appreciable percentage growth inhibition underwent further dose response analysis allowing for the calculation of a GI$_{50}$ value. This value is the drug concentration at which cell growth is 50%

11

FULL PAPER

inhibited based on the difference between the optical density values on day 0 and those at the end of drug exposure.[24, 25]

Molecular docking

Molecular docking simulations were performed using the default settings of Molecular Operating Environment (MOE). The human S100A2 crystal structure (RCSB ID: 2RGI) was prepared in MOE using the protonate 3D function: the system was protonated, partial charges added, and minimization performed. The designed 3D structures were built using the software molecular builder and were subjected to conformational analysis using a stochastic search approach. Each conformational library was docked into the p53 binding groove of the S100A2 homodimer using "Triangle Matcher" as the placement method and "London dG" as the scoring function for the initial ligand placement. The top 20 poses were then refined with the GBVI/WSA scoring function. The highest ranked pose for each compound was relaxed in the binding groove using LigX energy minimisation. Analysis and visualisation of the docking output, such as identification of hydrogen bonds, steric clashes, hydrophobic interactions, or π-π interactions, were performed in MOE.[24, 25]

References

[1] Wirth, M.; Mahboobi, S.; Kra mer, O. H.; Schneider, G. Concepts to Target MYC in Pancreatic Cancer. *Mol. Cancer Ther.* **2016**, *15*, 1792–1798.

[2] Rahib, L.; Smith, B. D.; Aizenberg, R.; Rosenzweig, A. B.; Fleshman, J. M.; Matrisian, L. M. Projecting Cancer Incidence and Deaths to 2030: The Unexpected Burden of Thyroid, Liver, and Pancreas Cancers in the United States. *Cancer Res.* **2014**, *74*, 2913–2921.

[3] https://www.canceraustralia.gov.au/publications-and-resources/cancer-australia-publications/pancreatic-cancer-fact-sheet. Types of Pancreatic Cancer Fact Sheet. **2014**, No. June 2014.

[4] Glenney, J. R. Jr.; Kindy, M. S.; Zokas, L. Isolation of a new member of the S100 protein family: amino acid sequence, tissue, and subcellular distribution. *J. Cell Biol.* **1989**, *108*, 569-578.

[5] Marrenholz, I.; Heizmann, C. W.; Fritz, G. S100 proteins in mouse and man: from evolution to function and pathology (including an update on nomenclature). *Biochem. Biophys. Res. Commun*. **2004**, *322*, 1111-1122.

[6] Deshpande, R.; Woods, T. L.; Fu, J.; Zhang, T.; Stoll, S. W.; Elder, J. T. Biochemical characterization of S100A2 in human keratinocytes: subcellular localization, dimerization, and oxidative cross-linking. *J. Invest. Dermatol.* **2000**, *115*, 477-485.

[7] Ilg, E. C.; Schafer, B. W.; Heizmann, C. W. Expression patterns of S100 calcium-binding proteins in human tumours. *Int. J. cancer.* 1996, 68, 325-332.

[8] Totti, S.; Vernardis, S. I.; Meira, L.; Pérez-Mancera, P. A.; Costello, E.; Greenhalf, W.; Palmer, D.; Neoptolemos, J.; Mantalaris, A.; Velliou, E. G. Designing a Bio-Inspired Biomimetic in Vitro System for the optimization of ex vivo studies of pancreatic cancer. *Drug Disc. Today* **2017**, *22*, 690–701.

[9] Mueller, A.; Schafer, B. W.; Ferrari, S.; Weibel, M.; Makek, M.; Hochli, M.; Heizmann, C. W. The calcium-binding protein S100A2 interacts with p53 and modulates its transcriptional activity. *J. Biol. Chem*. **2005**, *280*, 29186-29193.

[10] Bhattacharya, S.; Bunick, C. G.; Chazin, W. J. Target selectivity in EF-hand calcium binding proteins. *Biochim. Biophys. Acta*, **2004**, *1742*, 69-79.

[11] Bresnick, A. R.; Weber, D. J.; Zimmer, D. B. S100 Proteins in Cancer. *Nat. Rev. Cancer* **2015**, *15*, 96–109.

[12] Fernandez-Fernandez, M. R.; Rutherford, T. J.; Frescht, A. R. Members of the S100 family bind p53 in two distinct ways. *Protein Sci.*, **2008**, *17*, 1663-1670.

[13] Van Dieck, J.; Fernandez-Fernandez, M. R.; Veprintsev, D. B.; Fersht, A. R. Modulation of the oligimerization state of p53 by differential binding of proteins of the S100 family to p53 monomers and tetramers. *J. Biol. Chem.,* **2009**, *284*, 13804-13811.

[14] Van Dieck, J.; Teufel, D. P.; Jaulent, A. M.; Fernandez-Fernandez, M. R.; Rutherford, T. J.; Wyslouch-Ciexszynska, A.; Fersht, A. R. Posttranslational modifications affect the interaction of S100 proteins with tumour suppressor p53. *J. Mol. Biol.*, **2009**, *394*, 922-930.

[15] Biankin, A. V.; Kench, J. G.; Colvin, E. K.; Segara, D.; Scarlett, C. J.; Nguyen, N. Q.; Chang, D. K.; Morey, A. L.; Lee, C. -S.; Pinese, M.; Kuo, S. C. L.; Susanto, J. M.; Cosman, P. H.; Lindeman, G. J.; Visvader, J. E.; Nguyen, T. V.; Merrett, N. D.; Warusavitarne, J.; Musgrove, E. A.; Henshall, S. M.; Sutherland, R. L.; NSW Pancreatic Cancer Network. Expression of S100A2 calcium-binding protein predicts response to pancreatomy for pancreatic cancer. *Gastroenterology*, **2009**, *137*, 558-568.

[16] Ohuchida, K.; Mizumoto, K.; Ishikawa, N.; Fujii, K.; Konomi, H.; Nagai, E.; Yamaguchi, K.; Tsuneyoshi, M.; Tanaka, M. The role of S100A6 in pancreatic cancer development and its clinical implications as a diagnostic marker and therapeutic target. *Clin. Cancer Res.* **2005**, *11*, 7785-7793.

[17] Ohuchinda, K.; Ohuchida, K.; Mizumoto, K.; Miyasaka, Y.; Yu, J.; Cui, L.; Yamaguchi, H.; Toma, H.; Takahata, S.; Sato, N.; Nagai, E.; Yamaguchi, K.; Tsuneyoshi, M.; Tanaka, M. Over-expression of S100A2 in pancreatic cancer corelates with progression and poor prognosis. *J. Pathol.* **2007**, *213*, 275-282.

[18] Hountis, P.; Mattaios, D.; Froudarkis, M.; Bouros, D.; Kakolyris, S.; S100A2 protein and non-small cell lung cancer. The dual role concept. *Tumour Biol.* **2014**, *35*, 7327-7333.

[19] Bailey, P.; Chang, D. K.; Nones, K.; Johns, A. L.; Patch, A. M.; Gingras, M. C.; Miller, D. K.; Christ, A. N.; Bruxner, T. J. C.; Quinn, M. C.; Nourse, C.; Murtaugh, L. C.; Harliwong, I.; Idrisoglu, S.; Manning, S.; Nourbakhsh, E.; Wani, S.; Fink, L.; Holmes, O.; Chin, V.; Anderson, M. J.; Kazakoff, S.; Leonard, C.; Newell, F.; Waddell, N.; Wood, S.; Xu, Q.; Wilson, P. J.; Cloonan, N.; Kassahn, K. S.; Taylor, D.; Quek, K.; Robertson, A.; Pantano, L.; Mincarelli, L.; Sanchez, L. N.; Evers, L.; Wu, J.; Pinese, M.; Cowley, M. J.; Jones, M. D.; Colvin, E. K.; Nagrial, A. M.; Humphrey, E. S.; Chantrill, L. A.; Mawson, A.; Humphris, J.; Chou, A.; Pajic, M.; Scarlett, C. J.; Pinho, A. V.; Giry-Laterriere, M.; Rooman, I.; Samra, J. S.; Kench, J. G.; Lovell, J. A.; Merrett, N. D.; Toon, C. W.; Epari, K.; Nguyen, N. Q.; Barbour, A.; Zeps, N.; Moran-Jones, K.; Jamieson, N. B.; Graham, J. S.; Duthie, F.; Oien, K.; Hair, J.; Grützmann, R.; Maitra, A.; Iacobuzio-Donahue, C. A.; Wolfgang, C. L.; Morgan, R. A.; Lawlor, R. T.; Corbo, V.; Bassi, C.; Rusev, B.; Capelli, P.; Salvia, R.; Tortora, G.; Mukhopadhyay, D.; Petersen, G. M.; Munzy, D. M.; Fisher, W. E.; Karim, S. A.; Eshleman, J. R.; Hruban, R. H.; Pilarsky, C.; Morton, J. P.; Sansom, O. J.; Scarpa, A.; Musgrove, E. A.; Bailey, U. M. H.; Hofmann, O.; Sutherland, R. L.; Wheeler, D. A.; Gill, A. J.; Gibbs, R. A.; Pearson, J. V.; Waddell, N.; Biankin, A. V.; Grimmond, S. M. Genomic Analyses Identify Molecular Subtypes of Pancreatic Cancer. *Nature* **2016**, *531*, 47–52.

[20] Dreyer, S.; Dreyer, S. B.; Pinese, M.; Jamieson, N. B.; Scarlett, C. J.; Colvin, E. K.; Pajic, M.; Johns, A. L.; Humphris, J. L.; Wu, J.; Cowley, M. J.; Chou, A.; Nagrial, A. M.; Merrett, N. D.; Gill, A. J.; Duthie, F.; Miller, D. K.; Cooke, S.; Aust, D.; Ru, Ã. P.; Kno, T.; Pilarsky, C.; Nguyen, N. Q.; Musgrove, E. A.; Chang, D. K. Precision Oncology in Surgery : Patient Selection for Operable Pancreatic Precision Oncology in Surgery Patient Selection for Operable Pancreatic Cancer. *Protein Sci.* **2018**, *17*, 1663–1670.

[21] Koch, M.; Fritz, G. The Structure of Ca2+-Loaded S100A2 at 1.3-Å Resolution. *FEBS J.* **2012**, *279*, 1799–1810.

[22] Tan, M.; Heizmann, C. W.; Guan, K.; Schafer, B. W.; Y, Y. S. Transcriptional Activation of the Human S100A2 Promoter by Wild-Type p53. *FEBS Lett.* **1999**, *445*, 265–268.

[23] Cossar, P. J.; Abdel-Hamid, M. K.; Ma, C.; Sakoff, J. A.; Trinh, T. N.; Gordon, C. P.; Lewis, P. J.; McCluskey, A. Small-Molecule Inhibitors of the NusB-NusE Protein-Protein Interaction with Antibiotic Activity. *ACS Omega.* **2017**, *2*, 3839–3857.

[24] Baker, J. R.; Gilbert, J.; Paula, S.; Zhu, X.; Sakoff, J. A.; McCluskey, A. Dichlorophenylacrylonitriles as AhR Ligands Displaying Selective Breast Cancer Cytotoxicity in Vitro. *ChemMedChem* **2018,** *13*, 1447-1458.

[25] Abdel-hamid, M. K.; Macgregor, K. A.; Odell, L. R.; Chau, N.; Mariana, A.; Whiting, A.; Robinson, J.; McCluskey, A. 1,8-Naphthalimide Derivatives: New Leads against Dynamin I GTPase Activity. *Org. Biomol. Chem.* **2015**, *13*, 8016–8028.

12

Acknowledgements

13

Entry for the Table of Contents
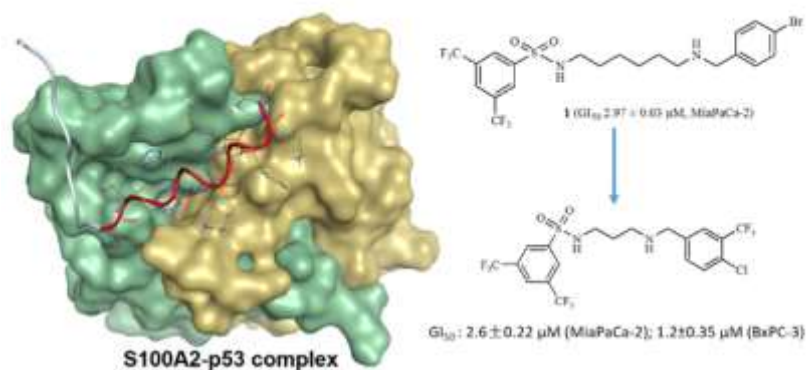
S100A2-p53 complex

Targeting the S100A2-p53 complex reveals novel pancreatic cancer cytotoxic specific small molecule inhibitors. Enhanced potency is noted against S100A2 containing PC cell lines MiaPaCa-2 and BxPC-3.

14